LA-9358-C
Conference

C.3

Los Alamos National Laboratory is operated by the University of California for the United States Department of Energy under contract W-7405-ENG-36.

Proceedings of the Los Alamos Neutrino Workshop

June 8-12, 1981

Los Alamos National Laboratory
Los Alamos, New Mexico 87545

This work was supported by the US Department of Energy, Office of Energy Research.

LA-9358-C
Conference

UC-34c
Issued: August 1982

Proceedings of the Los Alamos Neutrino Workshop

June 8-12, 1981

Compiled and Edited by
F. Boehm*
G. J. Stephenson Jr.

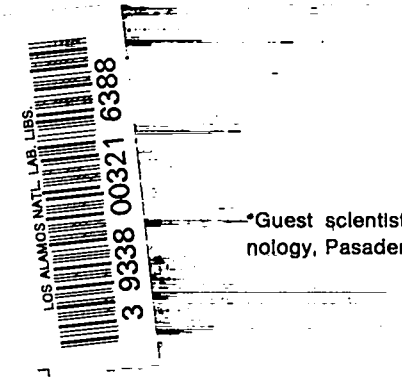

*Guest scientist. Permanent address: Physics Department, California Institute of Technology, Pasadena, CA 91125.

Los Alamos National Laboratory
Los Alamos, New Mexico 87545

CONTENTS

PROCEEDINGS OF THE LOS ALAMOS NEUTRINO WORKSHOP

June 8 - 12, 1981

Compiled and Edited by

F. Boehm and G. J. Stephenson Jr.

ABSTRACT

A workshop on neutrino physics was held at Los Alamos from June 8 to 12, 1981. The material presented has been provided in part by the organizers, in part by the chairmen of the working sessions. Closing date for contributions was October 1981.
Copies of this report can be obtained from G. J. Stephenson Jr., Physics Division, Los Alamos National Laboratory, Los Alamos, NM 87545.

I. INTRODUCTION

For many years it has been clear that the intense medium energy proton beam at the Clinton P. Anderson Meson Physics Facility (LAMPF) could be a copious source of neutrinos for the study of neutrino nucleus interactions. A major drawback to many such experiments is the long duty factor of the machine, leading to serious cosmic ray backgrounds. The advent of a Proton Storage Ring (PSR) on LAMPF beam line D, with its concomitant reduction of the duty factor to about 3×10^{-6}, makes it possible to consider several experiments that would otherwise be impossible. These facts were noted, discussed, and documented in the Proceedings of the LAMPF Program Options Workshop held in August 1979.

Meanwhile, the interest in neutrino properties, especially in masses and in possible flavor mixings, has become even more acute. Experimental evidence has been reported hinting at the existence of neutrino oscillations, as well as finite neutrino mass. Other experiments, although not confirming oscillations, give stringent limits for neutrino masses and mixing parameters. Several proposals have been generated to search for oscillation phenomena at LAMPF, both at the beam stop and on beam line D. Other questions related to neutrino couplings to electrons, nucleons, and nuclei through charged and neutral current interactions remain important unresolved issues.

With this in mind, the Los Alamos National Laboratory, through the auspices of its Physics, Meson Physics, and Theoretical Divisions, convened a Los Alamos Neutrino Workshop during June 8 - June 12, 1981. The purpose of the workshop was to review the physics that could be studied at a dedicated neutrino facility, and to delineate the feasibility of such a facility at Los Alamos. The workshop was attended by physicists from the nuclear physics and particle physics communities. The participants were asked to join various working groups with interlocking membership that dealt with the following topics: particle physics and nuclear physics problems of interest, calculation of neutrino-nucleus cross sections and neutrino fluxes, detector design, cost, and other uses of pulsed beams.

The charge to the participants, the programs, the list of participants, and the working group compositions are presented in the Appendix.

The report is organized as follows. In the second section two theoretical plenary talks by P. Ramond and T. W. Donnelly discussing neutrino experiments are reproduced. (Another presentation by A. K. Mann reviewing current activities at high-energy accelerators is not included.) The third section contains the working group reports and is followed by a brief conclusion.

II. PLENARY TALKS

THE CASE FOR NEUTRINO OSCILLATIONS

P. Ramond

Physics Department, University of Florida, Gainesville, FL 32611

The building of a machine capable of producing an intense, well-calibrated beam of muon neutrinos is regarded by particle physicists with keen interest because of its ability of studying neutrino oscillations.

The possibility of neutrino oscillations has long been recognized, but it was not made necessary on theoretical or experimental grounds; one knew that oscillations could be avoided if neutrinos were massless, and this was easily done by the conservation of lepton number. The idea of grand unification has led physicists to question the existence (at higher energies) of global conservation laws. The prime examples are baryon-number conservation, which prevents proton decay, and lepton-number conservation, which keeps neutrinos massless, and therefore free of oscillations. The detection of proton decay and neutrino oscillations would therefore be an indirect indication of the idea of Grand Unification, and therefore of paramount importance.

Neutrino oscillations occur when neutrinos acquire mass in such a way that the neutrino mass eigenstates do not match the (neutrino) eigenstates produced by the weak interactions. We shall study the ways in which neutrinos can get mass, first at the level of the standard $SU_2 \times U_1$ model, then at the level of its Grand Unification Generalizations.

We start by discussing neutrinos in the standard model. The left-handed electron- (muon or tau) neutrino is best described in terms of a two-component left-handed (Weyl) spinor, ν_L, which represents a left-handed particle and its right-handed antiparticle, thus conserving CP in first approximation. This is to be contrasted with a charged particle (such as the electron), which is described by two such fields, e_L and e_R, conserving C and P separately. The left-handed fields, ν_{eL} and e_L, form a weak isodoublet ($I_W = 1/2$) and ν_L has $I_w = +1/2$. The standard model interactions involving neutrinos are of the form $\nu_L e_L$, $\nu_L \nu_L$, and $\nu_L e_R$. Hence, if we assign lepton number L=1 to all the fields, these interactions conserve L. Note that the electron mass

term $e_L e_R$ + c.c conserves L as well, and it violates weak isospin by $\Delta I_w = 1/2$, because e_R is a weak singlet. The left-handed neutrino field can have a mass, the so-called Majorana mass of the form $\nu_L \sigma_2 \nu_L$ (in the Weyl representation); it violates weak isospin as $\Delta I_w = 1$. However, this Majorana mass clearly violates lepton number L by two units. Hence, no neutrino Majorana mass can develop in a theory with L conservation. In the standard model, the Higgs particle is taken to be a weak doublet with L=0, which couples the right-handed electron field to the weak doublet (ν_L, e_L). When it acquires a vacuum expectation value, it gives the electron its (Dirac) mass and gives the famous relation

$$\frac{M_w}{M_z \cos\theta_w} = 1 \quad , \tag{1}$$

relating the Weinberg angle to the W- and Z-boson masses. The standard model conserves L and neutrinos cannot acquire masses. However, one can easily generalize it in order to get a massive neutrino by breaking L explicitly or spontaneously in the Lagrangian. The easiest is to add a Higgs field, which is a weak isotriplet ($\Delta I_w = 1$) and has L = -2. The extra Yukawa coupling would then be of the form

$$(\nu_L^T \; e_L^T)\tau_2 \vec{\tau} \begin{matrix} \nu_L \\ e_L \end{matrix} \cdot \vec{\phi} \quad , \tag{2}$$

where $\vec{\phi} = (\phi^0, \phi^+, \phi^{++})$ is complex to preserve electric charge. If the field ϕ^0 gets a mass, it is known to be very small in comparison to that of the Higgs doublet because the relation (1) is experimentally good to 3-5%. However, it generates a Majorana mass for the neutrino. An interesting signature of this coupling would be the appearance of a doubly charged (exotic) Higgs particle in the $e^+ e^+$ channel. However, this is only one of many ways to obtain massive neutrinos in the standard model. For instance, the introduction of explicit L-violating terms in the Hamiltonian will liberate the neutrino mass and induce it sooner or later in perturbation theory. (Remember that, in the standard model, L-conservation is the only

symmetry that prevents a Majorana neutrino mass.) Hence, to go further one has to blend in extra theoretical prejudices. We use those of Grand Unification, which, loosely speaking, says that at some scale one cannot tell a quark from a lepton, which means that there exist vector (gauge) particles that cause transitions between leptons and quarks. Assign baryon number B=1/3(-1/3) for quark (antiquark) and B=0 for lepton; also set L=0 for quarks and antiquarks. Thus a vector boson that mediates lepton-antiquark transition has B=1/3 and L=1 and is a color triplet. Another vector boson color triplet changes an antiquark into a quark and has B = -2/3, L=0. In the simplest Grand Unified Theory these two vector bosons are the same, thus violating B and L separately. However, because these two have the same value of B-L = -2/3, B-L is conserved and, because the neutrino Majorana mass has B-L = 2, neutrinos are still massless in the simplest Grand Unified Model, although it allows for proton decay, as is well known.

Grand Unified Models beyond SU_5 introduce fermions not found in the standard model and these fermions pave the way for B-L violation. In fact, a characteristic of all models beyond SU_5, such as SO_{10}, E_6 is their extra neutral fermions.

In the following, without showing any particular model, we will analyze in terms of the standard model what happens in five different types of generalizations for the neutral lepton content of the theory.

The first type of generalization involves more of the usual neutrinos; the mass matrix is now purely $\Delta I_w=1$:

$$(\nu_L^{1/2})(\Delta I_w=1)(\nu_L^{1/2}) \quad , \tag{3}$$

where $\nu_L^{1/2}$ stands for the normal neutrinos (three in the standard model). Then, as discussed earlier, these neutrinos can be made massless by imposing L-conservation.

In the second case we have an extra neutrino with $I_w^3 = -1/2$ such as would appear in a theory with V+A currents. Then the most general mass matrix in the neutral lepton sector looks like

$$(\nu_L^{1/2} \quad N_L^{-1/2}) \qquad \begin{pmatrix} \Delta I_w = 1 & \Delta I_w = 0,1 \\ \Delta I_w = 0,\ 1 & \Delta I_w = 1 \end{pmatrix} \begin{pmatrix} \nu_L^{1/2} \\ N_L^{-1/2} \end{pmatrix} \quad . \quad (4)$$

In the above, $N_L^{-1/2}$ stands for the new type neutrino with $I_w = -1/2$. The off-diagonal elements contain the so-called Dirac mass and the diagonal elements are the Majorana masses. Because the mass matrix contains a $\Delta I_w = 0$ component, it has to be understood why it is of the same order of magnitude as the $\Delta I_w = 1$ component. Because the matrix has no zero eigenvalues, the neutrinos are naturally massive.

The third type of generalization involves adding neutral leptons that are mute ($I_w = 0$) under weak interactions. We denote them by N_L^o. The neutral lepton mass matrix now looks like

$$(\nu_L^{1/2} \quad N_L^o) \qquad \begin{pmatrix} \Delta I_w = 1 & \Delta I_w = 1/2 \\ \Delta I_w = 1/2 & \Delta I_w = 0 \end{pmatrix} \qquad \begin{pmatrix} \nu_L^{1/2} \\ N_L^o \end{pmatrix} \quad . \quad (5)$$

Note the appearance of $\Delta I_w = 1/2$ entries in this mass matrix. Barring any global conservation laws, these entries will be of the order of the charged leptons and quark masses, say $\sim$1 GeV. Hence the resulting Majorana mass for the garden variety neutrino will be unacceptably large!

The way out is to give the $\Delta I_w = 0$ entry a <u>very</u> large value M. The mass matrix will then look like

$$\begin{pmatrix} 0 & m \\ m & M, \end{pmatrix} \quad (6)$$

and will have a small eigenvalue

$$m_\nu \sim m \frac{m}{M} \quad , \quad (7)$$

that is, depressed from the usual mass by the ratio of the $\Delta I_w=1/2$ to $\Delta I_w=0$ scales. In Grand Unified Theories, such as SO_{10}, the $\Delta I_w=0$ scale is $\sim 10^{15}$GeV, yielding the requisite suppression.

The fourth kind of generalization involves both types of weakly interacting extra neutrinos $N_L^{1/2}$ and $N_L^{-1/2}$ self-conjugate fermion). The mass matrix now looks like

$$\left(\nu_L^{1/2} \quad N_L^{1/2} \quad N_L^{-1/2}\right) \begin{pmatrix} \Delta I_w=1 & & \Delta I_w=0,1 \\ \Delta I_w=0,1 & & \Delta I_w=1 \end{pmatrix} \begin{pmatrix} \nu_L^{1/2} \\ N_L^{1/2} \\ N_L^{-1/2} \end{pmatrix}. \tag{8}$$

In the absence of the $\Delta I_w=1$ component, the new matrix becomes

$$\begin{pmatrix} 0 & 0 & A \\ 0 & 0 & B \\ A & B & 0 \end{pmatrix}, \tag{9}$$

which, upon diagonalization, gives a massless left-handed neutrino and a massive Dirac neutral lepton of mass of the order of the $\Delta I_w=0$ mixing.

Lastly, one can have a combination of the last two cases, such as in the Grand Unified Theory based on E_6. In the above we have not included generalizations to neutral fermions with I_w = 1, 3/2, ...assignments since they would involve exotic charge assignments for their (weak) partners.

Thus, when we have in addition to the usual neutrinos a self-conjugate fermion (that is, like $N_L^{1/2}$ and $N_L^{-1/2}$), it is more natural to preserve the masslessness of the neutrino; whereas, when the extra fermions are nonself-conjugate (that is, an odd number of extra fermions), it becomes rather difficult to preserve neutrino masslessness.

Can we now offer some guesses as to the numerical value of neutrino masses and mixing angles? In general, after diagonalization of the charged and neutral lepton mass matrices, the charged current density will look like

$$\left(e_L^+ \quad \mu_L^+ \quad \tau_L^+\right)\left(U\right)\left(T\right)\begin{pmatrix}\nu_{RL}\\ \nu_{\mu L}\\ \nu_{\tau L}\end{pmatrix} \quad + \ldots \quad , \tag{10}$$

where U is a unitary 3x3 matrix coming from the diagonalization of the charged lepton mass matrix, and T is a 3x3 matrix (not necessarily unitary) obtained by diagonalizing the neutral lepton mass matrix. (The unwritten part of the density (10) involves transitions of other particles.) If we take the ansatz between mass and mixing angles

$$\tan^2\theta_{ij} \sim \frac{m_i}{m_j} \quad , \tag{11}$$

and

$$\frac{m_e}{m_\mu} \sim \frac{1}{200} \; ; \qquad \frac{m_\mu}{m_\tau} \sim \frac{1}{20} \, , \tag{12}$$

we see that the U matrix does not mix appreciably the electron into the other two leptons, and provides a Cabibbo-like mixing between μ and τ. The form of T is much less definite because we do not know any neutrino masses. So we take an example based on SO_{10} (the third case discussed above). The neutral mass matrix is

$$\begin{pmatrix}M^1 & M^{1/2}\\ M^{1/2} & M^0\end{pmatrix}, \tag{13}$$

where $M^{\Delta I_w}$ are 3x3 matrices (for three families). Set the strengths for $M^{\Delta I_w}$ as follows:

$$\begin{aligned} \Delta I_w = 0 \quad &\sim \quad m_x \\ \Delta I_w = -1/2 \quad &\sim \quad m_w \equiv \epsilon m_x \quad , \\ \Delta I_w = 1 \quad &\sim \quad \epsilon^2 m_x \end{aligned} \tag{14}$$

where ϵ is the hierarchy parameter. We rewrite the matrix (13) as

$$\begin{pmatrix} \epsilon^2 M^1 & \epsilon M^{1/2} \\ \epsilon M^{1/2} & M^0 \end{pmatrix} \quad , \tag{15}$$

where all M are of the same order. Then the neutral fermion mass matrix is given by

$$\left(M^1\right) + \left(M^{1/2}\right)^T \left(\frac{1}{M^0}\right) \left(M^{1/2}\right) = T^T D T \quad , \tag{16}$$

where T is the matrix appearing in (10) and D is a diagonal matrix with the neutrino masses as entries. The point of this exercise is to note that the physically relevant parameters (mixing parameters in T, mass parameters in D) are determined from the knowledge of M^1, $M^{1/2}$, and M^0. Now $M^{1/2}$ can, under some general assumptions, be related to the charge 2/3 mass matrix (this happens in SO_{10}), but M^1 and M^0 are not directly related to known physics. In some schemes (where M^0 is a perturbation on the Grand Unification scale) it can be argued that M^1 can be neglected in (16), but this still leaves the matrix M^0. So, life is very complicated. Still, one can make educated guesses based on specific Grand Unified Models. One obtains, more often than not, a <u>very</u> light ν_e and much heavier but comparable ν_μ and ν_τ:

$$\frac{m_{\nu_e}}{m_{\nu_\mu}} \sim 10^{-6} \; ; \; \frac{m_{\nu_\mu}}{m_{\nu_\tau}} \lesssim 1 \quad . \tag{17}$$

Furthermore, one finds very little mixing between ν_e and ν_μ or ν_τ, but large mixing between ν_μ and ν_τ. None of these results are

ironclad, but they seem to be easier to obtain, using the greatest naïvete. Hence, they seem to indicate that ν_e-ν_μ oscillations will be all but impossible to detect while ν_μ-ν_τ oscillations would be more apparent.

Now with a "low-energy" machine, such results indicate that one should first look for the extinction of the ν_μ beam and then later for ν_μ-ν_e oscillations. Moreover, these are just theories that are not directly coordinated with known phenomenology, and it is impossible to gauge their validity. For the moment, one would be satisfied with the findings of ν-oscillations, irrespective of which way they occur. This would reinforce our theoretical beliefs that global conservation laws are not fundamental, and as such would be as important as the discovery of proton decay.

Acknowledgment

I wish to thank Profs. F. Boehm and G. Stephenson Jr. for asking me to participate in the stimulating workshop. I also wish to thank the Aspen Center for Physics where the above was written.

HIGHLIGHTS OF NUCLEAR PHYSICS WITH NEUTRINOS

T. W. Donnelly

Center for Theoretical Physics,

Massachusetts Institute of Technology

Cambridge, MA 02139

The subject of electromagnetic and weak interactions is discussed in many places, including several review articles[1-4] that I have used in preparing this talk on nuclear physics with neutrinos. In particular I have drawn heavily on the material presented in Ref. 4 in which both charged and neutral current interactions are discussed and have employed the notation used in that work. The basic processes involved here are indicated diagrammatically in Fig. 1. These include: in Fig. 1a, electromagnetic interactions, namely, electron scattering and the special subclass, real-photon reactions (the former has $q \geq \omega$, where $q = |\vec{q}|$ is the three-momentum transfer and ω is the energy transfer, whereas the latter are restricted to the real-photon line $q = \omega$); in Fig. 1b, the "conventional" weak interaction processes, β-decay and charged lepton capture; in Fig. 1c, charge-changing neutrino reactions; in Fig. 1d, neutral-current neutrino scattering; and in Fig. 1e, electron scattering by the neutral current weak interaction. These interactions are mediated by exchange of the bosons γ, $W^{\pm}$ and Z^0. As we believe that we understand the interactions of the leptons with these bosons, the focus of such studies of semileptonic electroweak interactions in nuclei is on the hadronic side and is contained in the initial state, $|i\rangle$, to final state, $|f\rangle$, matrix elements of the appropriate operators,* specifically, $\hat{J}_\mu$, the electromagnetic current, $\hat{J}^{(+)}_\mu$, the charge-changing weak interaction current, and $\hat{J}^{(0)}_\mu$, the neutral-weak interaction current. Note that the same current operator, $\hat{J}_\mu$, enters in electromagnetic electron scattering and in real-photon reactions (that is, the same physics is involved). However, in the former it is possible to fix ω, for example to excite a given state in the nucleus, and to vary q over all values such

*Following the notation of Refs. 1-4, a second-quantized nuclear operator is indicated with a caret. Furthermore, h=c=1 is employed throughout.

that $q \geq \omega$ [that is, to map out an electromagnetic form factor $F(q)$], whereas in the latter, only one point on the form factor is measured, namely the $q=\omega$ point. So also in the processes shown in Figs. 1c-e, in principle it is possible to map out complete weak interaction form factors at fixed ω. However, as for the real-photon processes, under the conditions in which most of our present understanding of weak interactions in nuclei has been obtained, that is by the "conventional" weak processes, shown in Fig. 1b, the available range of momentum transfer q is severely limited. In β-decay, the four-momentum transfer is time-like, $q_\mu = q^2 - \omega^2 \leq 0$, so $q \leq \omega$. Now even a very high-energy nuclear β-decay reaction has $\omega < 20$ MeV, whereas a measure of when the momentum transfer is large or small is some typical nuclear value Q, say the Fermi momentum $Q \sim k_F \sim 200 - 250$ MeV. So in β-decay we are restricted to the low-q limit (or long wavelength limit, LWL) in which $q/Q \ll 1$. In charged lepton capture the momentum transfer $q \sim m_\ell - \omega$, where m_ℓ is the lepton mass (electron or muon). In electron capture we again have $q/Q \ll 1$, although in muon capture typically $q \sim 80$-100 MeV. Thus, in the "conventional" weak interaction processes only two separate momentum regions are explored, the low-q long wavelength region and the region around 80-100 MeV. Neutrino reactions (at least in principle) have the potential to explore the complete weak interaction form factors and not just those restricted, rather low-q regions.

Let us begin a discussion of the complete class of electroweak processes in nuclei by considering transitions between states $|i\rangle$ and $|f\rangle$ that are characterized by angular momentum J, parity π, and discrete energies E_i and E_f (specific examples are considered below). The differential cross sections (that is, differential in the lepton scattering angles) are given by:

$$\frac{d\sigma}{d\Omega} = \sigma_o F^2(q,\omega,\theta) \ , \tag{1}$$

where θ is the scattering angle (say between the incident neutrino and the exiting muon in the reaction (ν_μ, μ^-)), where σ_o is the elementary cross section (for example, the Mott cross section in electron scattering), and where $F^2(q,\omega,\theta)$ is a nuclear form factor. Expressions of this form may be obtained for all of the electroweak processes discussed here[1-4].

The form factors may be expressed in terms of matrix elements of specific angular momentum and isospin multipole projections of the currents (see Appendix B for the general discussion):

$$F(q,\omega,\theta) \sim \langle f|[\text{projections of } \hat{J}_\mu,\ J_\mu^{(\pm)} \text{ or } J_\mu^{(0)}]|i\rangle \quad . \tag{2}$$

By ignoring the isospin content for a moment, we have two basic types of currents to deal with here, a vector (V) current, J_μ (for all of the processes) and an axial-vector(A) current, J_μ^5 (for the weak interaction, but not for the electromagnetic interaction; the "5" indicates the extra γ_5 in the elementary axial-vector current, see Eq. (5b) below). As we are dealing with four-vectors, we then have eight basic types of multipoles listed in Table I.

TABLE I: MULTIPOLE OPERATORS

	V	parity	A	parity
$\mu = 0$	$\hat{M}_{JMJ}$	N	$\hat{M}^5_{JMJ}$	U
$\mu = 3$ (longitudinal)	$\hat{L}_{JMJ}$	N	$\hat{L}^5_{JMJ}$	U
$\mu = 1,2$ (transverse)	$\hat{T}^{el}_{JMJ}$	N	$\hat{T}^{el5}_{JMJ}$	U
	$\hat{T}^{mag}_{JMJ}$	N	$\hat{T}^{mag\ 5}_{JMJ}$	N

N = natural parity, $(-)^J$; U = unnatural parity, $(-)^{J+1}$

The details of such multipole decompositions of the currents are given in Refs. 1-4. In particular we usually assume that the vector current is conserved as in the case of electromagnetic interactions and, through the Conserved Vector Current (CVC) hypothesis, that the vector part of the weak interaction current is the same conserved current. With this assumption the longitudinal multipole, $\hat{L}$, may be related to the "charge" multipole, $\hat{M}$, and so

dropped from the list, leaving seven basic types of multipoles. Including the isospin content we must deal with multipoles labelled TM_T, where $T=M_T=0$ for isoscalar transitions (electromagnetic and neutral current weak interactions); $T=1$, $M_T=0$ for isovector neutral current processes (electromagnetics and weak); and $T=1$, $M_T=\pm 1$ for isovector charge-changing weak interaction processes (see Ref. 4 for the general isospin content).

As a specific example for orientational purposes, consider a transition from the ground state of ^{12}C, $J^\pi T=0^+ 0$ to the 15.11-MeV-excited state in ^{12}C having $J^\pi T=1^+ 1$, where both states have $M_T=0$. Only one multipole contributes, $\hat{T}^{mag}_{JMJ;TMT}$, with $J=1$, $T=1$, $M_T=0$; that is, we are discussing an M1 transition. Now the ground states of ^{12}B and ^{12}N also have $J^\pi T=1^+ 1$, however, now with $M_T=-1$ and $+1$, respectively. Thus in the charge-changing weak interaction processes we have the multipoles $\hat{T}^{mag}_{JMJ;TMT}$, $\hat{M}^5_{JMJ;TMT}$, $\hat{L}^5_{JMJ;TMT}$ and $T^{el5}_{JMJ;TMT}$, with $J=1$, $T=1$, $M_T = -1$ and $+1$, respectively. Furthermore, in the neutral current weak processes we have again these same four multipole operators, but now with $M_T = 0$. The relationship among these electroweak processes is illustrated in Fig. 2. We shall return to this important example a little later.

Now these multipole operators may be decomposed in the following way:

$$\hat{T}_X = \hat{T}_X^{(1)} + \hat{T}_X^{(2)} + \cdots \qquad (3)$$

where $\hat{T}_X$ stands for any one of the seven (or eight) basic operators in Table I, with X labeling the angular momentum and isospin content. Here $\hat{T}_X^{(1)} \sim a_2^\dagger a_1$ is a one-body operator (that is, it changes the quantum numbers of nucleons in the nucleus one-at-a-time from 1 to 2), $\hat{T}_X^{(2)} \sim a_4^\dagger a_3^\dagger a_2 a_1$ is a two-body operator [that is, it changes the quantum numbers of two nucleons in the nucleus from (1,2) to (3,4), etc.; see Ref. 5)]. Usually the one-body contributions dominate over the two-body, etc., contributions, where the latter include the effects of meson-exchange currents (see Refs. 6 and 7 for discussions of MEC effects in electromagnetic interactions). Thus, for the present purposes we shall restrict our attention entirely to the one-body operators, $(\hat{T}^1_X)$. For these an exact statement may be made:

$$<f|\hat{T}^{(1)}_X|i> = \sum_{\alpha\alpha'} <\alpha|T^{(1)}_X|a'> \psi^{(fi)}_X(\alpha\alpha') \ , \tag{4a}$$

where on the left-hand side is the many-body nuclear matrix element required in the nuclear electroweak form factor. This in general involves initial and final nuclear states with arbitrarily complicated many particle-many hole configurations. The right-hand side contains an expansion in single-particle matrix elements, where $\alpha \leftrightarrow \{n\ell jm_j, 1/2m_t\}$ is a complete set of single-particle quantum numbers and where the c-numbers $\psi^{(fi)}_X(\alpha\alpha')$ are one-body density matrix elements in which are buried all the complexities of the nuclear many-body problem. If we truncate the sums over α and α' to a finite model space (and we do this for example in performing shell model calculations for the nuclear states), then a finite (frequently quite small) set of numbers $\psi^{(fi)}_X(\alpha\alpha')$ characterizes the nuclear dynamics content for this specific transition. In fact we shall assume that isospin is a good quantum number, in which case we may deal with matrix elements reduced in angular momentum and isospin spaces. Then the above equation becomes

$$<f\|\hat{T}^{(1)}_{J;T}(q)\|i> = \sum_{a\alpha} <a\|T^{(1)}_{J;T}(q)\|a'> \psi^{(fi)}_{J;T}(aa') \ , \tag{4b}$$

where the symbols $\|\ \|$ denote the doubly reduced matrix elements and where $a \leftrightarrow [n\ell j, 1/2]$, that is, the single-particle quantum numbers other than m_j and m_t. Presuming that the single-particle matrix elements are known within some model space (we return to this below), then the following procedure may be tried:

(1) For a well-studied process such as electron scattering measurements of cross sections lead to form factors [Eq. (1)] and hence to the many-body reduced matrix elements as functions of q for the appropriate operators [that is, to the left-hand side of Eq. (4b)].

(2) These may be expanded in a set of single-particle matrix elements within some model space with expansion coefficents being the one-body density matrices ψ.

(3) Now the relationship may be turned around for less well-known processes such as the weak interaction reactions. The same set of density matrices ψ are used, but now with the appropriate weak interaction operators and their single-particle matrix elements. This yields the many-body reduced matrix elements, the form factors and hence the weak interaction cross sections. In other words, the point of this procedure is to bury our lack of knowledge of nuclear dynamics in the minimum number of relevant quantities (the one-body density matrices) and to let a known process such as electron scattering determine them to the extent that this is possible. In a sense one is "calibrating a specific nuclear transition" by following these steps and by using all the good quantum numbers available. By choosing appropriate nuclear transitions one uses the nucleus as a "filter" to study selectively different pieces of the electroweak interaction. Several examples of following these procedures are reviewed in Ref. 4 (see also the references contained therein).

Let us return now to the form of the single-particle matrix elements in Eq. 4. Using general principles such as Lorentz covariance, parity, and time-reversal invariance and conservation of isospin we may write[4]:

$$< \vec{k}'\lambda';m_t'|J_\mu(0)_{TMT}|\vec{k}\lambda;m_t>$$

$$= i\bar{u}(\vec{k}'\lambda';m_t')\left[F_1^{(T)}\gamma_\mu + F_2^{(T)}\sigma_{\mu\nu}q_\nu + iF_s^{(T)}q_\mu\right] I_T^{MT}\, u(\vec{k}\lambda;m_t) \qquad (5a)$$

$$< \vec{k}'\lambda';m_t'|J_\mu^5(0)_{TMT}|\vec{k}\lambda;m_t>$$

$$= iu(\vec{k}'\lambda';m_t')[F_A^{(T)}\gamma_5\gamma_\mu - iF_p^{(T)}\gamma_5 q_\mu - F_T^{(T)}\gamma_5\sigma_{\mu\nu}q_\nu]I_T^{MT}\, u(\vec{k}\lambda;m_t) \qquad (5b)$$

for the free single-nucleon matrix elements of a vector (5a) and axial-vector (5b) current. Here the nucleon states are labelled by momentum $\vec{k}$, helicity λ, and isospin projection $m_t=\pm 1/2$.. The isospin content of the operator is contained in[4]

$$I_T^{MT} \equiv 1/2 \times \begin{matrix} 1 & T = 0, M_T = 0 \\ T_0 = T_3 & T = 1, M_T = 0 \\ T_{\pm 1} = \frac{1}{2}(T_1 \pm iT_2) & T = 1, M_T = \pm 1 \end{matrix} . \quad (6)$$

The single-nucleon form factors F_1, F_2, F_S, F_A, F_P, and F_T (Dirac, Pauli, induced scalar, axial-vector, induced pseudoscalar and induced tensor, respectively) are all functions of four-momentum transfer q_μ^2. We shall assume throughout that the vector current is conserved (see above), in which case F_S=0. Furthermore, we take only first-class currents to be non-zero, so that F_T=0 as well. We adopt a strong form of CVC and assume that there is only one vector current for both electromagnetic and weak interaction processes. That is, we take only a single set of couplings $[F_1^{(T)}, F_2^{(T)}, F_A^{(T)}, F_P^{(T)}, T=0,1]$ and construct the physical currents through the relations:

$$(J_\mu(0))_{em} = J_\mu(0)_{0,0} + J_\mu(0)_{1,0} \quad (7a)$$

$$(J_\mu(0))_{wk}^{(\pm)} = J_\mu(0)_{1,\pm 1} + J_\mu^5(0)_{1,\pm 1} \quad (7b)$$

$$(J_\mu(0))_{wk}^{(0)} = \beta_v^{(0)} J_\mu(0)_{0,0} + \beta_A^{(0)} J_\mu^5(0)_{0,0} \quad (7c)$$

$$+ \beta_v^{(1)} J_\mu(0)_{1,0} + \beta_A^{(1)} J_\mu^5(0)_{1,0}$$

for the electromagnetic, charge-changing weak and neutral weak interaction currents respectively. Here the neutral current couplings $\beta_V^{(T)}$, $\beta_A^{(T)}$, T = 0,1 depend on the underlying gauge theory model of the electroweak interactions.[4] In particular, for the standard W-S-GIM model (see Ref. 4 for a brief introduction to gauge theory models), we have

$$\beta_v^{(T)} = \alpha_v^{(T)} - \alpha_{em} \ , \ T = 0,1$$
$$\beta_A^{(T)} = \alpha_A^{(T)} \ , \ T = 0,1 \qquad , \qquad (8)$$

with

$$\alpha_v^{(0)} = \alpha_A^{(0)} = 0$$
$$\alpha_v^{(1)} = \alpha_A^{(1)} = 1 \qquad (9)$$
$$\alpha_{em} = 2 \sin^2\theta_w \ ,$$

so that, for example, there is no axial-vector isoscalar neutral current weak interaction coupling. We return to this point below.

As a final step in making the connection to nuclear physics one takes the nonrelativistic limit of the single-nucleon expressions (Eq. 5) and employs the appropriate single-particle wave functions (not plane waves as in Eq. 5, but more commonly harmonic oscillator wave functions[8] or Hartree-Fock wave functions or some approximation to them). This yields the single-particle matrix elements needed on the right-hand side of Eq. 4 in terms of the elementary single-nucleon couplings F_1, F_2, F_A, and F_P.

Let us now turn to several examples of these concepts and the resulting predictions for neutrino reactions, (ν_ℓ,ℓ^-), $(\bar{\nu}_\ell,\ell^+)$, where ℓ = e or μ, and neutrino scattering, (ν_ℓ,ν'_ℓ), $(\bar{\nu}_\ell,\bar{\nu}'_\ell)$. The A=6 example constitutes a (see Fig. 3) much-studied simple case where these ideas have been explored.[9] The adjustment of the density matrix elements ψ (in this case, re-expressed in terms of wave function amplitude coefficients, see Ref. 9) permits an excellent fit to the electron scattering data to be made [a fit including high-q (ee') data is shown in Fig. 4]. Having determined the required one-body density matrix elements, it is possible to predict the analog weak interaction rates. In fact, the β-decay and μ-capture rates predicted are in good agreement with the measured values,[9,11] giving us confidence that

the neutrino-induced processes can be predicted with good precision (to perhaps 10-15% in this case). The charge-changing and neutral current neutrino cross sections are shown in Figs. 5 and 6, respectively.

Another classic example is the A=12 system (see Fig. 2). Here a one-body density matrix analysis of the type described above[4] yields the neutrino cross sections shown in Figs. 7 and 8.

Other examples show a similar behavior (see Ref. 4 for discussion of several other cases). Two such worth mentioning in passing are the ^{7}Li case (ground state and 0.478 keV first-excited state) that may serve as an excellent neutral current excitation case for reactor neutrinos[12] and, secondly, the special case of $0^{+} \to 0^{-}$ transitions,[14] as in the A=16 system, where the neutrino reaction cross sections are sensitively dependent on the induced tensor second-class current coupling, F_T (see Eq. 5b).

An important general feature also worth mentioning at this point is to note the low-q or long wavelength behavior of the various multipoles (the allowedness, in usual β-decay terminology). This is discussed in Refs. 4 and 15 in some detail. The important point here in the present discussion is that for inelastic neutrino scattering the axial-vector dipole dominates, whereas for elastic neutrino scattering (because of the coherence in this case) the vector monopole dominates. These are the analogs of the familiar Gamow-Teller and Fermi β-decay allowed multipoles.[15] Thus, at not too large momentum transfer (say $q/Q<1$, using the above estimate of $Q \sim k_F \sim$ 200-250 MeV), one has a special situation: for inelastic scattering an M1 transition is predominately axial-vector; for elastic scattering the vector current dominates. In the former case, by selecting the isospin quantum numbers[4,15] we may selectively study the isoscalar axial-vector and isovector axial-vector couplings, $\beta_A^{(0)}$ and $\beta_A^{(1)}$ in Eqs. 7c and 8. Note that, in the standard model (see Eq. 9), the former vanishes: Such an isoscalar M1 transition could provide a sensitive test of the underlying gauge theory model couplings.[4,15]

Turning to the other allowed multipole, the vector monopole or "Fermi" matrix element, we see that the cross section for elastic neutrino scattering[4] is proportional to A^2 (just as elastic electron scattering is proportional to Z^2). However, the target recoil energy is proportional to A^{-1} and for A too large becomes too small (for given neutrino energy) to

detect. Thus, although very heavy targets have, relatively speaking, very large neutrino cross sections (and this is relevant in astrophysics in collapsing massive stars), at the neutrino energies of interest here the interest in elastic scattering centers on rather light nuclei. The elastic neutrino scattering cross section $\sigma(\nu,\omega)$ may be expressed as a function of the neutrino energy ν, and the recoil energy ω (or equivalently, the momentum transfer q, where $\omega=q^2/2M_{target}$ or the scattering angle θ). For a given value of ν there is a maximum recoil energy, ω_M (corresponding to $\theta=180^o$), whereas for practical reasons there is a minimum recoil energy, ω_m below which the recoiling nucleus cannot be detected ($0 \leq \omega_m \leq \omega_M$). Thus, the appropriate measure of the magnitude of the elastic neutrino scattering cross section is the integrated cross section

$$\sigma(\nu,\omega_m) = \int_{\omega_m}^{\omega_M} d\omega\, \sigma(\nu,\omega). \tag{10}$$

In particular, the case of ^{4}He seems to be of special experimental interest,[15] and in Fig. 9 the elastic neutrino cross section is shown. This is proportional to $(\beta_V^{(0)})^2 = (\alpha_V^{(0)}-2\sin^2\theta_w)^2$ (see Eq. 8 and Ref. 4) and so provides still another test of the underlying gauge theory model (in the standard model, $\alpha_V^{(0)}=0$; see Eq. 9). It would be very nice to see the nuclear coherence effect demonstrated for the neutral current weak interaction. This constitutes a test of <u>isoscalar</u> CVC.

As a final example here let me turn from discussions of <u>exclusive</u> reactions in which the kinematic variables are presumed to be well enough known that only a single discrete nuclear transition is involved to <u>inclusive</u> reactions where a range of nuclear excitations is integrated over to obtain the measured cross section. With a spectrum of neutrino energies from a neutrino facility this will frequently be the case in fact. In Fig. 10 the A=12 situation is indicated schematically. To obtain the total neutrino cross section it is necessary to sum over the giant resonance excitations and also the higher energy quasi-elastic region. This is just the situation that

occurs in inelastic electron scattering at these energies (see Fig. 10). The problem is that the models used for the quasi-elastic region (usually the Fermi gas model) are known to be rather poor at these values of q and ω for electron scattering. Thus whereas the giant resonance excitation region (see Fig. 11) is probably quite well accounted for by the ODW calculation[13] (that is, to perhaps 10-30%), the higher excitation energy region is not so well understood. As this inclusive reaction is the one used in neutrino detection in a class of neutrino oscillation experiments it is important to do the best job possible on predicting the cross section; this will likely occupy most of the time for deliberations by the Working Group on Nuclear Cross Sections.

In conclusion, there are many examples of exclusive nuclear neutrino reactions that test specific parts of the electroweak current. The primary use of nuclear targets, as against the nucleon, is likely to be this ability to select, or "filter out," specific pieces of the interaction. Two exceptions, however, come to mind: (1) It would be of interest to demonstrate the nuclear coherence seen in elastic neutrino scattering as discussed above, and likely the ^{4}He case is the one favored; and (2) there may be a time when questions of axial-vector meson-exchange current effects (many-body nuclear effects) can be addressed, perhaps in the case of deuteron-neutrino disintegration.

Rather than state more specific conclusions here as to which targets and which specific transitions deserve the most attention, I will defer such judgments to the Working Group on Nuclear Physics with Neutrinos where they can be arrived at collectively.

REFERENCES

1. T. deForest, Jr., and J. D. Walecka, Adv. Phys. 15, 1 (1966).

2. T. W. Donnelly and J. D. Walecka, Ann. Rev. Nucl. Sci. 25, 329 (1975).

3. J. D. Walecka, in "Muon Physics," Vol. 2, V. W. Hughes and C. S. Wu, Eds. (Academic Press, N.Y., 1975) p. 113.

4. T. W. Donnelly and R. D. Peccei, Phys. Reports 50, 1 (1979).

5. A. L. Fetter and J. D. Walecka, "Quantum Theory of Many-Particle Systems," (McGraw-Hill, N.Y., 1971).

6. J. Dubach, J. H. Koch, and T. W. Donnelly, Nucl. Phys. A271, 279 (1976).

7. T. W. Donnelly, J. W. Van Orden, T. deForest, Jr., and W. C. Hermans, Phys. Letts. 76B, 393 (1978); J. W. Van Orden, and T. W. Donnelly, Ann. Phys. 131, 451 (1981).

8. T. W. Donnelly and W. C. Haxton, Atomic Data and Nucl. Data Tables 23, 103 (1979); 25, 1 (1980).

9. T. W. Donnelly and J. D. Walecka, Phys. Lett. 44B, 330 (1973).

10. J. C. Bergstrom, U. Deutschmann, and R. Neuhausen, Nucl. Phys. A327, 439 (1979).

11. J. B. Cammarata and T. W. Donnelly, Nucl. Phys. A267, 365 (1976).

12. T. W. Donnelly, D. Hitlin, M. Schwartz, J. D. Walecka, and S. J. Wiesner, Phys. Lett. 49B, 8 (1974).

13. J. S. O'Connell, T. W. Donnelly, and J. D. Walecka, Phys. Rev. C6, 719 (1972).

14. T. W. Donnelly and J. D. Walecka, Phys Lett. 41B, 275 (1972).

15. T. W. Donnelly and R. D. Peccei, Phys. Lett. 65B, 196 (1976).

16. H. Chen and F. Reinees, UCI-Neutrino Report No. 31 (1979).

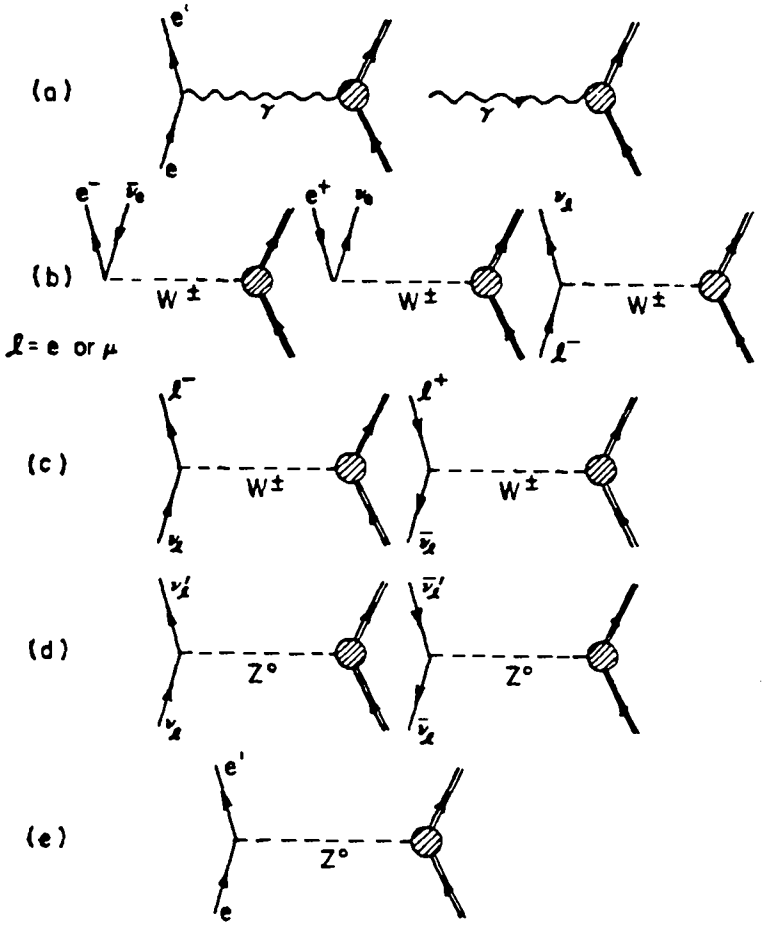

Fig. 1. Electroweak interaction processes. The heavy lines indicate a nucleus proceeding from an initial state i to a final state f. In the neutral current processes (a,d,e) the same nuclear system is involved; in the charge-changing reactions (b,c), neighboring nuclei differing by one unit in charge are involved.

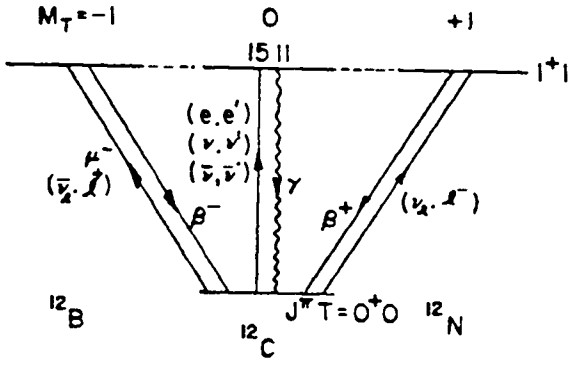

Fig. 2. Electroweak interaction processes in the A = 12 system.

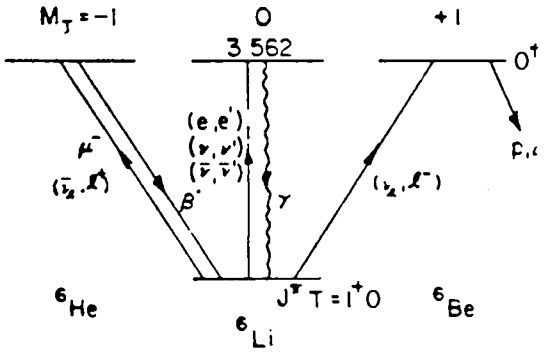

Fig. 3. Electroweak interaction processes in the A = 6 system.

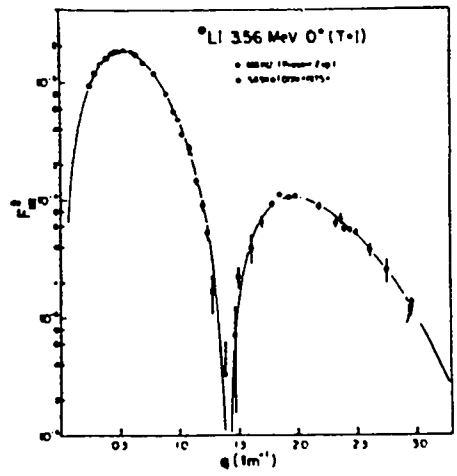

Fig. 4. Electron scattering form factor for the $1^+0 \rightarrow 0^+1$ (3.56 MeV) transition in ^{6}Li (from Ref. 10). The fit is obtained as described in the text.

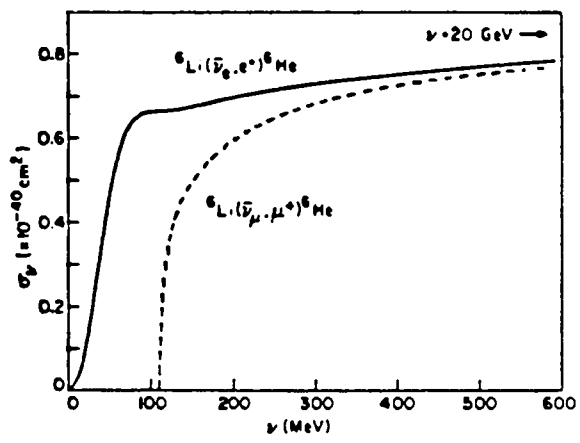

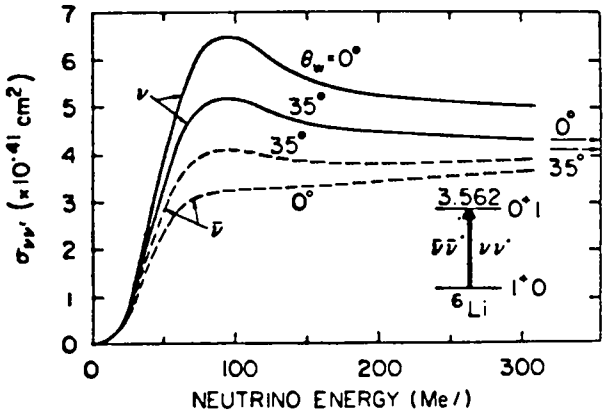

Figs. 5 and 6. Charge-changing and neutral current neutrino reactions in the A = 6 system (from Refs. 9 and 12, respectively). For the neutrino scattering calculations $\theta_W = 35^o$ was employed in Ref. 12, whereas 29^o is the currently accepted value.

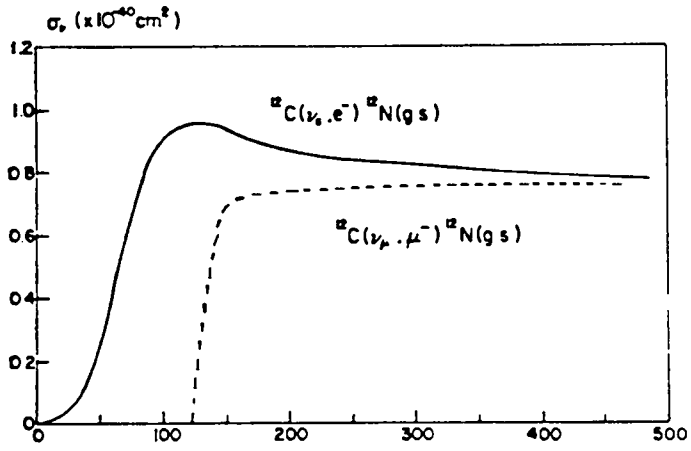

Figs. 7 and 8. Charge-changing and neutral current neutrino reactions in the A = 12 system (redrawn from the work of Ref. 13 and from Ref. 12, respectively). For the neutrino scattering calculations $\theta_W = 35^\circ$ was employed in Ref. 12, whereas 29° is the currently accepted value.

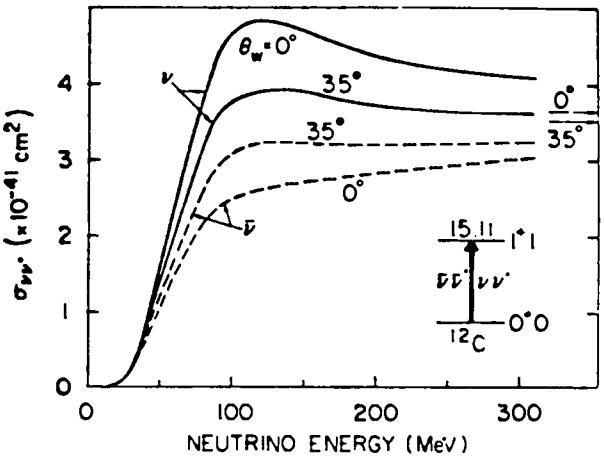

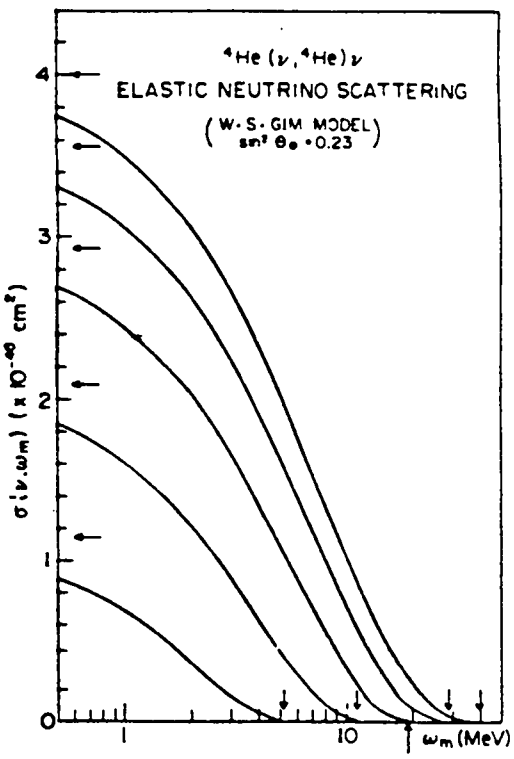

Fig. 9. Elastic neutrino scattering from ^{4}He. The integrated cross section $\sigma(\nu,\omega_m)$ is shown (see text, Eq. 10, and Appendix B. The curves proceeding from uppermost to lower correspond to ν = 300, 250, 200, 150, and 100 MeV neutrino energy. The arrows along the horizontal axis indicate the maximum recoil energies, δ_M, while the arrows along the vertical axis indicate tl e values of the cross sections reached if $\omega_m = 0$, that is, the total integrated cross sections.

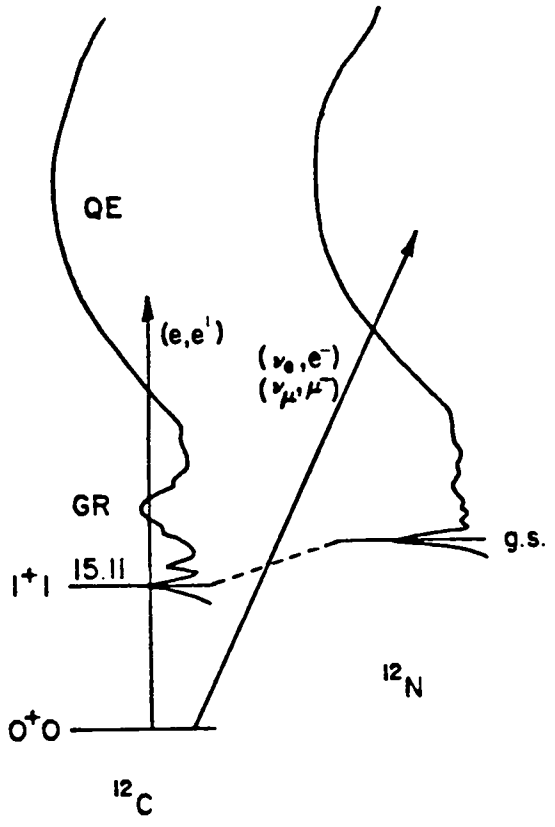

Fig. 10. Inelastic electroweak interactions in the A = 12 system. The 1^+1 15.11 MeV state of ^{12}C and its analog, the ground state of ^{12}N are shown. The region in which particle-hole states are excited, the giant resonance (GR) region is shown, as is the quasielastic (QE) region. These have analogs in the charge-changing neutrino reactions that connect ^{12}C to excited states of ^{12}N.

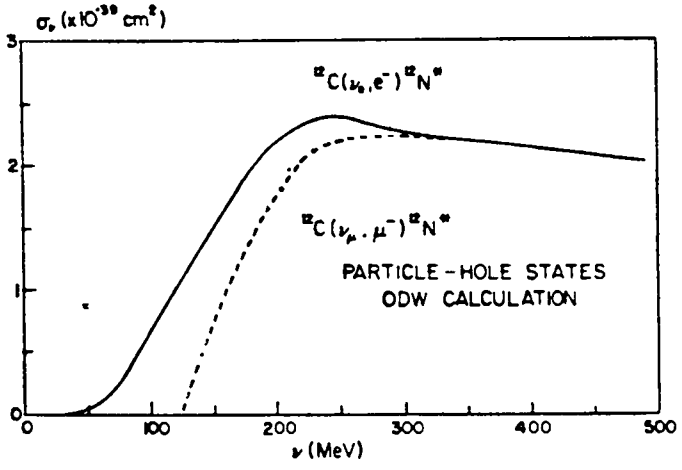

Fig. 11. Charge-changing neutrino reactions in the A = 12 system (redrawn from Ref. 13). Here the strength has been summed for the particle-hole states in the GR resonance region (roughly the first 15 MeV of excitation energy in ^{12}N). The one-body density matrices adopted here have been adjusted to produce a good fit to the (e,e') data.

WORKING GROUP ON PARTICLE PHYSICS

P. Ramond (Chairman), B. Barrish, F. Boehm, H. Chen, T. Goldman

A. Mann, T. Romanowsky, R. Slansky

This subcommittee discussed fundamental problems in particle physics with neutrinos in the 100-200 MeV range that would become available at the proposed facility.

Some of the unique properties of the facility were recognized and they are (1) high-ν flux, (2) short duty cycle and thus low cosmic-ray background, (3) availability of intense ν_e beams available from a "μ bottle."

These characteristics are necessary ingredients for the pursuit of the experiments sketched below. For convenience we classify the issues into the following subtitles

(A) Neutrino Oscillations

(B) Precision Determinations of Parameters in Low-Energy Neutrino Scattering

(C) ν_e Physics.

A. Neutrino Oscillations

Recently, good bounds for some oscillation parameters have become available from reanalyses of bubble chamber data from CERN and Fermilab, as well as from work at ILL-Grenoble, as summarized in Table 1. Nevertheless, studies with high sensitivity for the channels

ν_μ disappearance [process (1)]

$\nu_\mu \to \nu_e$ [process (2)]

remain an open issue and constitute an exciting task, well suited for the neutrino facility.

According to the LAMPF proposal 638 (Dombeck et al.) a sensitivity for process (1) and (2), respectively, of

$\Delta^2 \sim 0.2\ eV^2$ (full mixing), $\sin^2 2\theta \sim 0.05$ (large Δ^2)

$\Delta^2 \sim 0.02\ eV^2$ (full mixing), $\sin^2 2\theta \sim 0.002$ (large Δ^2)

should be attainable, with the "standard conditions" described below.

From a theoretical point of view it can be argued that ν_μ disappearance represents a promising candidate for finding oscillations (see Sec. II, P. Ramond, this report). However, it should not be forgotten that at the present time it is impossible to make any predictions corroborated by known physics. Clearly, if evidence for oscillations is found, a wide field of important questions will open up.

Although this is an issue of great importance, it should be kept in mind that the rather long delay (5-6 years) until results would be available will not pass unchallenged.

At present Brookhaven is considering oscillation experiments. According to A. Mann, the augmented E734 group, using two detectors at 100 m and 850 m, plans to perform a ν_μ-ν_e as well as ν_μ disappearance experiment with sensitivity limits quoted in Table I. If approved, data should be forthcoming in three or four years. The disappearance experiment will use both known flux values and charge-to-neutral current ratio.

Also, at CERN an experiment has been approved using BEBC and the 28 GeV PS beam that will be capable of exploring very small mixing angles (see Table I). Compared to the limits for high energy data from CERN and Fermilab, also shown in Table I, the proposed BEBC experiment, because of the lower neutrino energy ($\sim$1 GeV), will be sensitive to small Δ^2 values.

It appears, however, that the experiment proposed by the Los Alamos group (proposal 638) has the highest sensitivity for both Δ^2 and mixing angle for the ν_μ-ν_e channel and thus remains a well-worthwhile undertaking.

B. Precision Determination of Low-Energy Parameters

Crucial tests of theoretical models are provided by precision measurement of elastic scattering cross sections for both the leptonic and hadronic processes of low momentum transfer:

$$\nu_e e \to \nu_e e, \qquad \nu_\mu e \to \nu_\mu e$$

$$\nu_e p \to \nu_e p, \qquad \nu_\mu p \to \nu_\mu p.$$

From a precise cross section a precise value of $\sin^2 \theta_w$ could be derived.

For illustrative purposes, using as "standard condition" parameters discussed elsewhere in the report of a 50-T detector and a muon-neutrino flux

of $2 \times 10^5/cm^2$-s at 50 m, one could expect event rates of ~0.1/day for ν_μ-e scattering. The corresponding rate for ν_μ-p is ~3/day and the rates for ν_e (from μ^+ at rest) are expected to be ~0.5/day. Note that this condition was chosen for ease of comparisons and is not optimized for Los Alamos energies. Actual counting rates will be higher.

The importance of such a determination is exemplified by the recent calculation by Marciano and Sirlin (P.R.L. 46, 162 (1981)) of

$$\sin^2\theta_w\,(\nu_\mu e,\ q^2 = 0) = 0.2104 + 0.006\ \ell n[0.4\ \text{GeV}/\Lambda_{MS}]$$

($\Lambda_{MS} \equiv$ QCD scale parameter),

and similar predictions for ν_μ-hadron and ν_ee scattering. To test this prediction is clearly of great importance. No such experimental determination exists to date. There are other calculations [Dawson, et al., PR D23, 2666 (1981); Antonelli and Maiani N.P. B186, 269 (1981)] that predict values agreeing to within 4% with the cited value.

Further, such a result could eventually be compared with similar results for high-energy processes, for which Marciano and Sirlin also give a prediction. More generally, a precise determination of $\sin^2\theta_w$ is of importance to further test the standard WS model and its extensions. Below the 3% level the q^2 variation of $\sin^2\theta_w$ can also be tested. (The theoretical uncertainty in the variation is much less than in the absolute value.)

C. ν_e Physics

At present ν_e physics at ~100 MeV and higher is an unexplored field (if we disregard some beam dump work at CERN and Fermilab). The ν_ee scattering experiment now being readied at LAMPF (Exp. 225) will provide the first information on cross sections from charged and neutral current channels. The interference term between the charged and neutral current is a unique feature testing the diagonal nature of the neutral current as well as the WS model. The neutrino facility offers the possibility of performing such an experiment at increased energy and improved background conditions.

A test of universality in neutral current processes is provided by comparing ν_ee and ν_μe scattering cross sections. Such tests have not yet been performed in leptonic systems, and have given only crude data for hardonic processes (ν_ed at reactor energies vs. ν_μ-hadron).

Conclusion

The subcommittee concludes that there is a broad and varied class of experiments accessible to the proposed facility that are of great interest to particle physics. For some of these experiments, the design goals of the facility provide better sensitivity to neutrino mixing parameters than are achievable by any other installations, whether existing or proposed. For a few cases, the capabilities of the proposed facility are unique.

Clarifying discussions with P. Herczeg and L. Wolfenstein are gratefully acknowledged.

TABLE I

Limits (90% C. L.) for Oscillation Parameters

Channel	Year	Lab	Proposal	Detector	Δ^2	Sensitivity (90% C. L.) (full mix) $\sin^2 2\theta$ (large Δ^2)
(-) (-) $\nu_\mu - \nu_e$	1978	CERN[1]		GARGAMELLE	1.0	0.06
	1980	LAMPF[2]	E31	6 t Water Cer	0.9	0.2
	1981	FNAL[3]	E388	15'BC	2.0	0.02
	1981	FNAL[4]	E53A	15'BC	0.6	0.006
	1981	CERN[5]		BEBC	1.7	0.01
	(1982)	LAMPF	E225	13 t CH	0.35	0.01
	(?)	LAMPF	E609	5 t Gd Sc	0.1	0.01
	(1984?)	BNL[6]	E734A	200 t CH	0.1	0.03
	(1984?)	LAMPF	E645	5 t, 15 t D_2O	0.06	0.01
	(1984?)	CERN[7]	PS	BEBC	0.1	0.02
	(1985?)	LAMPF	E638	50 t CH	0.02	0.002
$\nu_\mu - \nu_\tau$	1981	FNAL[4]	E53A	15'BC	3.0	0.06
	1931	FNAL[8]	E531	emul.	3.5	0.03
	1981	CERN[5]		BEBC	6	0.05
$\nu_e - \nu_\tau$	1981	FNAL[4]	E53A	15'BC	8	0.6
ν_μ-disappearance	(1982)	FNAL[9]	701	300 t, 1000t Fe Sc	10-1000	0.05
	(1984?)	BNL[6]	E734A	200 t CH	0.2	0.1
	(1984?)	LAMPF	E645	5 t, 15 t D_2O	0.2	0.05
	(1984?)	CERN[10]	CDHS	1400 t Fe	0.25	0.2
	(1985)	LAMPF	E638	50 t CH	0.2	0.05
ν_e-disappearance	1980	LAMPF	E31	6 t Water Cer	2.5	0.5
	1980	GRENOBLE[11]	Reactor	0.4 t Sc, ^3He	0.15	0.3
	1981	CERN[5]		BEBC	10	0.07
	1982	GÖSGEN-SIN[11]	Reactor	0.4 t Sc, ^3He	0.01	0.1
	(1984?)	LAMPF	E645	5 t, 15 t D_2O	0.3	0.1

References to Table I

1. J. Blietschau et al., Nucl. Phys. B 133, 205 (1978).

2. P. Nemethy et al., Phys. Rev. D 23, 262 (1981).

3. Quoted by H. Chen, APS Baltimore (1981).

4. J. Baltay, in Neutrino Oscillation Workshop, Brookhaven, BNL 51380, p. 301 (1981).

5. O. Erriquez et al., Phys. Lett. 102B, 73 (1981).

6. BNL Proposal, BNL-Brown-KEK-Osaka-Penn-Stony Brook-Tokyo-UCI Collaboration, August 1981, and private communication A. Mann.

7. Private communication by A. Mann and V. L. Telegdi.

8. T. Kondo, Proc. Neutrino Miniconference, Telemark, Wis., p. 24 (1981).

9. FNAL-Columbia-CIT-Chicago-Rochester-Rockefeller Collaboration.

10. Private communication by H. Chen.

11. H. Kwon et al., Phys. Rev. D 24, 1097 (1981).

WORKING GROUP ON NUCLEAR PHYSICS WITH NEUTRINOS

T. Donnelly (Chairman), F. Boehm, D. Bryman, G. Garvey, A. McDonald,

R. McKeown, J. O'Connell, R. Robertson

The following is a summary of the conclusions reached by Nuclear Physics Group on the subject of nuclear physics with neutrinos to be addressed with the planned neutrino facility. In other material provided for the workshop[1-4] details of the reactions are considered and expanded upon, and more complete references to previously published work are given. The present section distills this material and states in summary form the conclusions reached at this time.

There are many examples of exclusive nuclear neutrino reactions that test specific parts of the electroweak current. The primary use of nuclear targets, as opposed to the nucleon, is likely to be this ability to select or "filter out" specific pieces of the interaction.[1] Two exceptions, however, come to mind: (1) It will be of interest to demonstrate the nuclear coherence seen in elastic neutrino scattering,[4] and likely the ^{4}He case is the one favored (see Fig. 9 and the accompanying discussion in Ref. 1); and (2) There may be a time when questions of axial-vector, meson-exchange current effects (many-body nuclear effects) can be addressed, perhaps in the case of deuteron-neutrino disintegration (see Fig. 1).

The specific priorities we see for nuclear physics with neutrinos are listed below.

I. FIRST PRIORITY REACTIONS

A. $p(\nu,p)\nu$, Elastic Neutrino Scattering to Test the Vector and Axial-Vector, Isoscalar and Isovector Parts of the Weak Neutral Current.

To disentangle the various pieces, both angular distributions of the recoil protons and the dependence of the cross-section on neutrino energy need to be explored as discussed in detail in Ref. 4. A measurement at 0°,

for example, determines exclusively the transverse piece of the cross section (see Table 1 of Ref. 1). Under "standard conditions" the event rate is expected to be about 3/day. The ability to study these features would be enhanced if the neutrinos had somewhat higher energies.

B. Neutrino Reactions With ^{2}H

$d(\nu,d)\nu$, elastic neutrino scattering to test the vector and axial-vector, purely isoscalar parts of the weak neutral current (the latter is zero in the W-S-GIM model). This reaction is discussed in some detail in Ref. 4, where it is shown that, as the recoil angle goes to zero, the reaction depends predominantly on the axial-vector coupling $\beta_{A}^{(0)}$. Hence an angular distribution will provide information on both isoscalar couplings.

$d(\nu,p)\nu n$, $d(\nu,n)\nu p$, $d(\nu,pn)\nu$, inelastic neutrino scattering, including potentially the last coincidence reaction. There is heightened sensitivity to the axial-vector, isovector weak neutral current here.

$d(\nu_{\ell}, \ell^{-})pp$, $d(\nu_{\ell},\ell^{-}p)p$, ℓ = e or μ, charge-changing deuterium neutrino-disintegration, including potentially the latter coincidence reaction to test the q-dependence of the charge-changing weak interaction. Results of calculations of the cross sections for the reactions $d(\nu_{\ell},\ell^{-})pp$ and $d(\nu_{\ell},\ell^{+})nn$, ℓ=e or μ are presented in Ref. 2.

II. SECOND PRIORITY REACTIONS

A. Inelastic Neutrino Excitation (ν,ν') Followed by De-Excitation of the Nucleus by γ,p,α ... Decay.

For example, the (ν,ν') excitation of the 15.11-MeV state of ^{12}C followed by γ-decay (see the discussion in Ref. 1, in particular Fig. 8). Another such example involves the (ν,ν') excitation of the 12.71-MeV state of ^{12}C also followed by γ-decay. The former transition tests only isovector neutral currents, although the latter is more sensitive to isoscalar neutral currents (there is a small amount of isospin mixing the the 12.71-MeV state). And, because at relatively low energies the axial-vector current dominates, again specific pieces of the weak neutral current may be studied. Expected event rate under "standard conditions" would be $\sim$0.5/day.

B. Coherent Elastic Scattering.

The prime example being $^4He(\nu, ^4He)\nu$ to (i) see the coherence demonstrated and (ii) measure the vector, isoscalar weak neutral current coupling. This constitutes a test of the extension of the usual isovector CVC hypothesis to include the isoscalar weak neutral current. This special case is discussed in Ref. 1 (see Fig. 9) and in more detail in Appendix B. Further experimental considerations may also be found in Ref. 4.

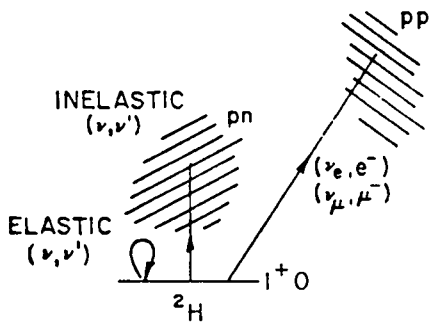

Fig. 1. Neutrino reactions in the A = 2 system.

REFERENCES

1. T. W. Donnelly, "Highlights of Nuclear Physics with Neutrinos," this report.

2. J. S. O'Connell, "Neutrino Reactions on the Deuteron," this report. See also J. S. O'Connell, "Neutrino Disintegration of the Deuteron at LAMPF Energies," Los Alamos Scientific Laboratory report LA-5175-MS (March 1973).

3. J. S. O'Connell, "Neutrino Reactions in the Fermi Gas Model," this report.

4. H. Chen and F. Reines, UCI-Neutrino Report No. 31 (1979).

WORKING GROUP ON NUCLEAR CROSS SECTIONS

J. S. O'Connell (Chairman), T. W. Donnelly, H. H. Chen,

R. L. Burman, B. Cortez

This working group was charged to study cross sections for neutrino-nucleus reactions. The charge particularly related to the calculation of certain inclusive cross sections that have direct bearing on the design of detectors that may be used with a neutrino facility. After extensive discussion of the issues involved, it fell to the chairman to carry out those calculations. The results are presented in the following two contributions by him.

NEUTRINO REACTIONS IN THE FERMI GAS MODEL

J. S. O'Connell
Center for Radiation Research
National Bureau of Standards
Washington, D.C. 20234

An estimate of the electron and muon production cross sections for 0-300 MeV neutrinos on nuclei can be made by employing the noninteracting Fermi gas model. This model gives good parameterizations of inelastic electron scattering in the quasi-free region and of photo-pion production in the delta region.

The $A(\nu,\ell)A$ cross section is written as

$$\frac{d^2\sigma_{\nu,\ell}}{d\Omega_\ell dE_\ell} = C \frac{d\sigma_N}{d\Omega_\ell} R(q,\omega) \quad , \tag{1}$$

where $\ell = e^{\pm}, \mu^{\pm}$, C = Z or N, and $d\sigma_N/d\Omega_\ell$ is the fundamental nucleon cross section. The kinematic variables are defined in Fig. 1 for the following reactions in nuclei:

$$\underset{-}{\nu}_e + n \rightarrow p + e^-$$

$$\nu_e + p \rightarrow n + e^+$$

$$\underset{-}{\nu}_\mu + n \rightarrow p + \mu^-$$

$$\nu_\mu + p \rightarrow n + \mu^+ \quad .$$

The cross section for the elementary reactions is[1]

$$\frac{d\sigma}{d\Omega}(\nu/\nu) = \frac{G^2 kE}{2\pi^2} \frac{1}{\left(1 + \frac{2\nu \sin^2\theta/2}{M}\right)} \times \left\{\left[F_1^2 + F_A^2 + \eta\left(2MF_2\right)^2\right] \cos^2\theta/2 \right. \tag{3}$$

$$+ 2\left[F_A^2(1+\eta) + \eta\left(F_1 + 2MF_2\right)^2\right] \sin^2\theta/2$$

$$\left. (-/+) \frac{2F_A}{M}\left(F_1 + 2MF_2\right)\left(q_\mu^2 \cos^2\theta/2 + q^2 \sin^2\theta/2\right)^{1/2} \sin\theta/2 \right\} \quad ,$$

with $\eta = \frac{q_\mu^2}{4M^2}$, $q_\mu^2 = q^2 - \omega^2$

$$F_1 = \left(1 + q_\mu^2/(855\ \text{MeV})^2\right)^{-2}$$

$$2MF_2 = 3.71\ F_1$$

$$F_A = -1.24\left(1 + q_\mu^2/(1000\ \text{MeV})^2\right)^{-1}$$

$$G = 1 \times 10^{-5}/M^2 \quad .$$

The nuclear response function in the nonrelativistic gas model is

$$R = \frac{3M}{4qP^3} \times \begin{cases} 2M\omega \text{ when } q < 2P_F \\ \qquad \text{and } \omega < \frac{qP_F}{M} - \frac{q^2}{2M} \\ \text{otherwise} \end{cases}$$

$$p_F^2 - \left(\frac{M\omega}{q} - \frac{q}{2}\right)^2 \quad .$$

The results for the nucleon cross sections and for nuclei with Fermi momentum p_F = 220 MeV/c and average nucleon separation energy E_B = 25 MeV typical of carbon or oxygen are shown in Figs. 2-5. These cross sections should be useful in estimating counting rates for experimental feasibility studies with broad band neutrino beams.

REFERENCES

1. J. D. Walecka, "Semileptonic Weak Interactions in Nuclei" in Muon Physics Vol. II. Ed. by V. W. Hughes and C. S. Wu, Academic Press 1975. See pp. 184-189.

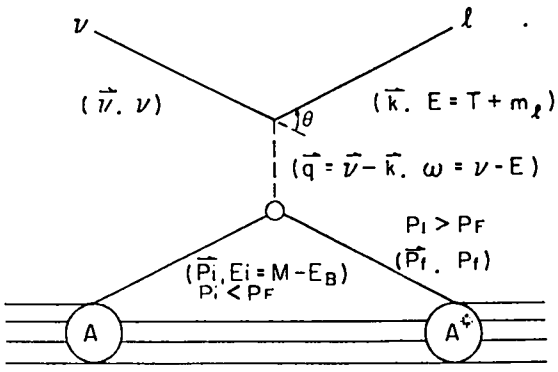

Fig. 1 Kinematic variables for neutrino production of electrons or muons on a nucleus.

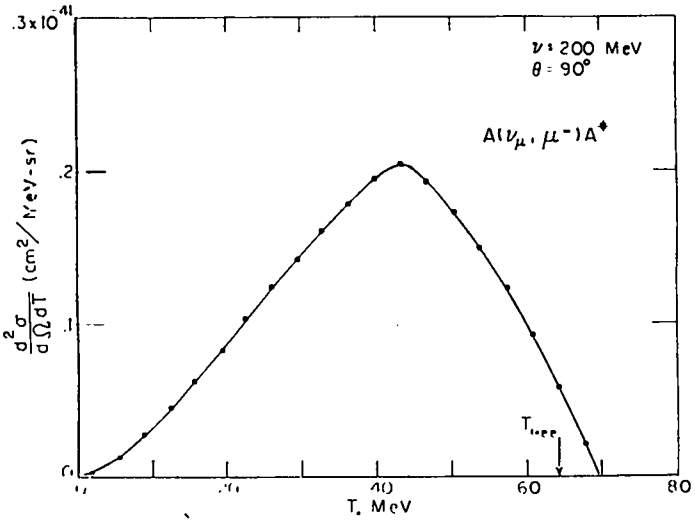

Fig. 2 Double differential charged current cross-section from light nuclei.

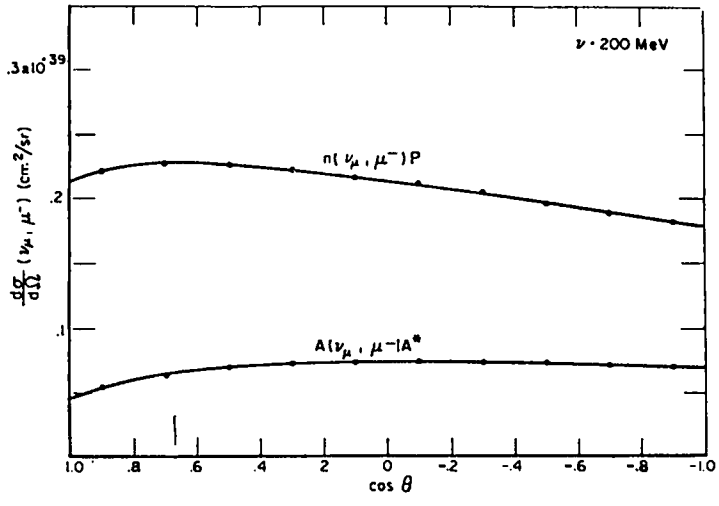

Fig. 3 Charged current cross-sections from the nucleon and a light nucleus.

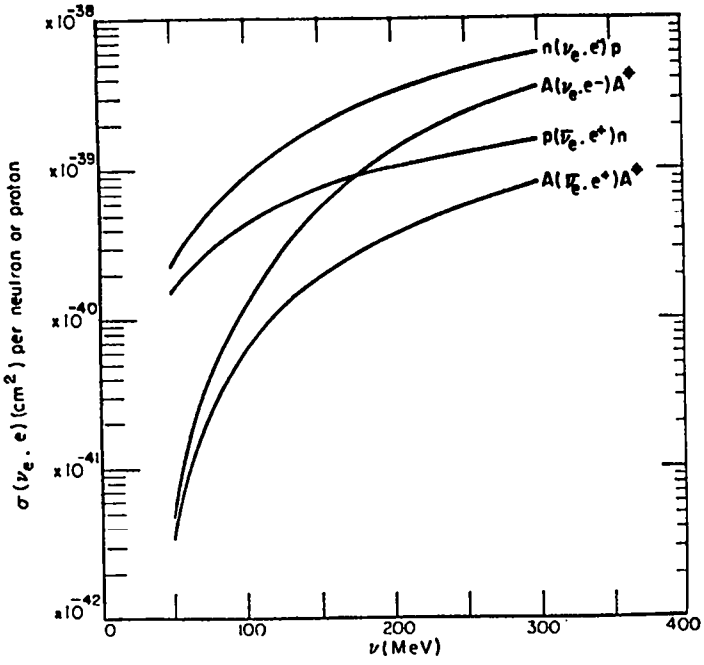

Fig. 4 Charged current cross-sections from nucleons and light nuclei.

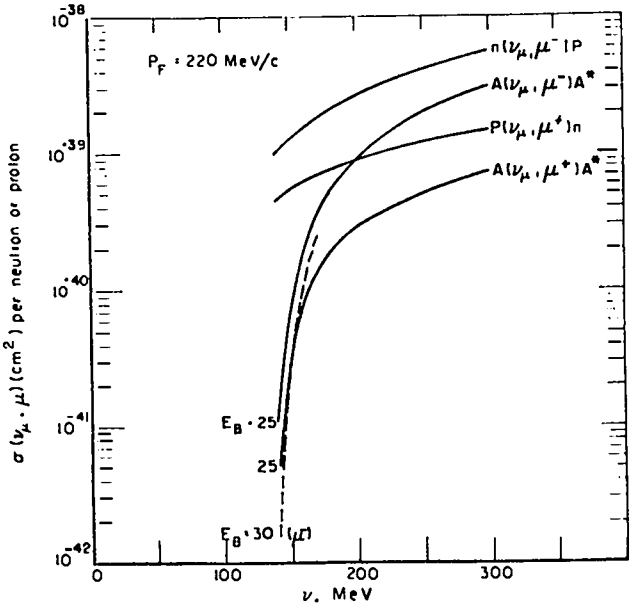

Fig. 5 Charged current cross-sections from nucleons and light nuclei.

NEUTRINO REACTIONS ON THE DEUTERON

J. S. O'Connell

Center for Radiation Research
National Bureau of Standards
Washington, D.C. 20234

A calculation of the cross sections of the charge-changing neutrino reactions

$$\begin{aligned} \bar{\nu}_e + D &\to 2p + e^- \\ \nu_e + D &\to 2n + e^+ \\ \bar{\nu}_\mu + D &\to 2p + \mu^- \\ \nu_\mu + D &\to 2n + \mu^+ \end{aligned} \qquad (1)$$

for the neutrino energy range 0-300 MeV can be made by using the elementary nucleon cross section together with model two-nucleon wave functions. The Yamaguchi[1] form (based on spin-dependent separable potentials) is convenient because it gives analytic transition amplitudes. This approach has proven successful in calculating[2] photopion production in deuterium.

The kinematic variables are defined in Fig. 1. The cross section is written as

$$\frac{d^2\sigma_{\nu\ell}}{d\Omega_\ell dE_\ell} = \frac{MP}{3}\left[|\langle\psi_s|\psi_D\rangle|^2 \frac{d\sigma_N^{SF}}{d\Omega} + 2|\langle\psi_t|\psi_D\rangle|^2 \frac{d\sigma^{NSF}}{d\Omega}\right] , \qquad (2)$$

where the free nucleon neutrino cross section $d\sigma/d\Omega$ is divided into its spin-flip (SF) and non-spin-flip (NSF) components[3]

$$\frac{d\sigma}{d\Omega}(\nu/\nu) = \frac{G^2 kE}{2\pi^2}\frac{1}{\left(1+\frac{2\nu\sin^2\theta/2}{M}\right)} \times \left\{\left[F_1^2 + F_A^2 + \eta(2MF_2)^2\right]\cos^2\theta/2 \right. \tag{3}$$

$$+ 2\left[F_A^2(1+\eta) + \eta\left(F_1+2MF_2\right)^2\right]\sin^2\theta/2$$

$$\left.(-/+)\frac{2F_A}{M}\left(F_1+2MF_2\right)\left(q_\mu^2\cos^2\theta/2 + q^2\sin^2\theta/2\right)^{1/2}\sin\theta/2\right\} ,$$

with $\eta = \frac{q_\mu^2}{4M^2}$, $q_\mu^2 = q^2 - \omega^2$

$$F_1 = \left(1 + q_\mu^2/(855\ \text{MeV})^2\right)^{-2}$$

$$2MF_2 = 3.71\ F_1$$

$$F_A = -1.24\left(1 + q_\mu^2/(1000\ \text{MeV})^2\right)^{-1}$$

$$G = 1 \times 10^{-5}/M^2 .$$

The NSF part is the F_1 term although the SF part is all the rest.

The two-nucleon transition amplitudes are: spin-singlet final states

$$\langle\psi_s|\psi_D\rangle = N\left\{\frac{1}{2\left(\alpha^2+p_-^2\right)\left(\beta_t+p_-^2\right)} + \frac{1}{2\left(\alpha^2+p_+^2\right)\left(\beta_t+p_+^2\right)}\right. \tag{4}$$

$$\left. + \frac{f_s/Q}{\left(\beta_t^2-\alpha^2\right)}\left[\tan^{-1}\left(\frac{(\beta_t-\alpha)Q}{(\beta_t-ip)(\alpha-ip)+Q^2}\right) - \tan^{-1}\left(\frac{(\beta_t-\alpha)Q}{(\beta_t+\beta_s)(\alpha+\beta_s)+Q^2}\right)\right]\right\} ,$$

and spin-triplet final states

$$\langle \psi_s | \psi_D \rangle = N \left\{ \frac{1}{2\left(\alpha^2+p_-^2\right)\left(\beta_t+p_-^2\right)} - \frac{1}{2\left(\alpha^2+p_+^2\right)\left(\beta_t^2+ p_+^2\right)} \right\} \quad , \qquad (5)$$

where

$$N^2 = 4\alpha\beta_t\left(\alpha+\beta_t\right)^3/\pi$$

$$\vec{p} = \vec{p}\,\vec{Q}, \quad \vec{Q} = \frac{1}{2}\left(\vec{\nu}-\vec{k}\right)$$

$$f_s = \left(p \cot \delta_s - ip\right)^{-1} = \left(e^{2i\delta_s} - 1\right)/2ip$$

$$p \cot \delta_s = -\frac{1}{a_s} + \frac{1}{2} r_o p^2 - P r_o^3 p^4 \quad .$$

The parameters used were:

$$\alpha = .232 \text{ fm}^{-1}, \; a_s = -17 \text{ fm}$$

$$\beta_t = 1.392 \text{ fm}^{-1}, \; \beta_s = 1.13 \text{ fm}^{-1}$$

$$P r_o^3 = -0.3838 \text{ fm}^3, \; r_o = 2.84 \text{ fm} \quad .$$

The total cross sections are shown in Figs. 2 and 3.

This finite range calculation improves upon and extends the neutrino energy range of a previous calculation[4] based on zero-range wave function. One expects corrections to the present results if better two-nucleon wave functions are used and from the addition of meson exchange currents to the single-nucleon amplitude. However the present results may prove useful in estimating counting rates in experimental feasibility studies with broad band neutrino beams.

REFERENCES

1. Y. Yamaguchi, Phys. Rev. 95, 1628 (1954).

2. E. T. Dressler, W. M. MacDonald, and J. S. O'Connell, Phys. Rev. C20, 267 (1979).

3. J. D. Walecka, "Semileptonic Weak Interactions in Nuclei" in Muon Physics, Vol. II, Ed. by V. W. Hughes and C. S. Wu, Academic Press 1975. See pp 184-189.

4. J. S. O'Connell, "Neutrino Dişintegration of the Deuteron at LAMPF Energies" (0-53 MeV) LA-5175-MS (1973).

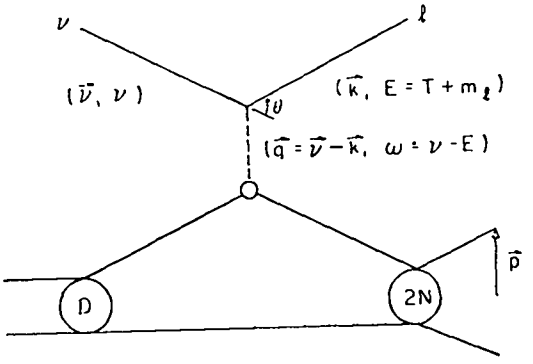

Fig. 1 Kinematic variables for neutrino disintegration of the deuteron with production of a charged lepton.

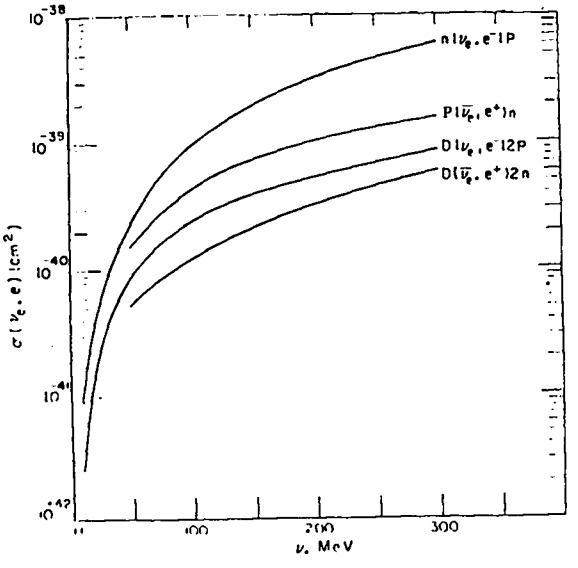

Fig. 2 Total charged-current cross-sections on the proton, neutron and deuteron with ν_e and $\bar{\nu}_e$.

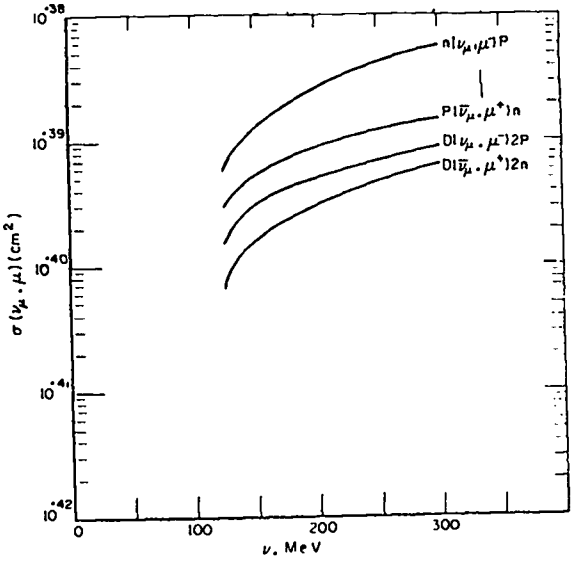

Fig. 3 Total charged-current cross-sections on the proton, neutron and deuteron with ν_μ and $\bar{\nu}_\mu$.

WORKING GROUP ON NEUTRINO FLUX CALCULATIONS

R. C. Slansky (Chairman), R. P. Redwine, T. W. Dombeck, T. D. Romanowski,

A. K. Mann, H. H. Chen, B. Cortez, G. T. Garvey

The working group was given the task of obtaining reliable neutrino flux calculations for a neutrino facility of the type planned at Los Alamos. Clearly, all parameters pertaining to the neutrino production rate, such as target, pion focusing, pion decay channel, and shielding configuration, must be optimized to achieve the largest flux possible.

The following input parameters were fixed as a "standard condition" and all flux values are expressed in terms of this choice, except when noted:

proton beam: 800 MeV, 100 μA

target: 40-cm-long carbon, 5-cm diam

decay channel: 30 m } Total target-dectector distance: 50 m

shielding: tuff, 20 m }

The "standard condition" also includes a 50-T detector.

Several members of the working group presented results of neutrino flux calculations, using various computer codes. The results are given in Table I.

It follows from these calculations that an average flux value of 2.7×10^5 cm^{-2}sec^{-1} is the best and most reliable estimate at this time.

The working group urges interested parties to improve and optimize these calculations. Optimization should take into account π-decay length and shielding density and geometry. A shorter decay length (12 m) and a dense steel shield (9 m) will improve the solid angle by a factor of $(50/19)^2 = 8.3$ but not significantly reduce the ν production yield.

A crucial ingredient for the neutrino flux calculation is the inclusive pion production cross section at small angles for protons on carbon and other materials. Besides the early work by Cochran et al. (730-MeV protons, 15°), little is known from experiment. Final evaluation of the flux parameters must await more comprehensive studies of pion production yields at 800 MeV, now in

progress at LAMPF. We strongly recommend that LAMPF management give full support to these measurements.

Further improvements should be obtainable with a pion focusing device. Work needs to be done in designing a focusing magnet and the working group recommends that the laboratory management assign this task to a special study group. The magnet should also allow charge selection (ν, $\bar{\nu}$ selection).

The feasibility of a muon storage device should be examined. Such a "muon bottle" would be a necessary requirement for the production of copious high energy ν_e beams. As envisaged throughout these discussions, the availability of ν_e beams constitutes an important and unique feature of a neutrino facility. The target area should be designed so as not to preclude the installation of such a storage device.

Finally, the working group supports further studies of proposals to accelerate protons beyond the present 800 MeV LAMPF energy. Clearly, important advantages can be reaped from higher energy protons. Not only will there be an increase in neutrino production rate and kinematic focusing, but, even more important, there will be a strong gain in event rate in certain detectors from the rapid increase in the charged-current cross section in this energy region. Similarly, studies aimed at increasing the proton current beyond the proposed 100 μA level should be encouraged.

TABLE I

Results of ν_μ Flux Calculations

Author	E_p(MeV)	Target	$\langle E_\nu(\text{MeV})\rangle$	Flux($cm^{-2}sec^{-1}$)
Wang[a]	730	40 cm Be	130	3.7×10^5
Cortez[b]	800	40 cm C	160	4.0×10^5
Dombeck[c]	800	33 cm C	149	2.6×10^5
Mann[d]	730	40 cm C	120	1.6×10^5
Hyman[e]	800	33 cm C	118	1.5×10^5

[a]R. C. Allen, H. Chen, and K. C. Wang, UCI, Internal Report, Neutrino #67 (1981).

[b]B. Cortez, private communication.

[c]T. Dombeck, private communication.

[d]A. Mann, private communication.

[e]L. G. Hyman and B. Musgrave, ANL-HEP-PR-81-18 and erratum June 26, 1981.

WORKING GROUP ON A GENERAL PURPOSE NEUTRINO DETECTOR FACILITY

B. C. Barish (Chairman), A. K. Mann, P. H. Steinberg, R. McKeown,

H. H. Chen, R. L. Burman, R. G. H. Robertson, T. D. Romanowski

The characteristics of a possible general purpose neutrino detector for the PSR have been investigated. The major design parameters for such a detector have been determined by reviewing the requirements to attain the physics goals discussed in this report. To scope the detector, we have only considered a facility that uses present day techniques. It should be noted that technical developments that would enable construction of a "totally active detector" (for example, liquid argon drift chamber) appear promising. Future technical work toward such a detector should be encouraged.

Overall, a neutrino detector must perform two functions: a) provide target medium for the neutrino interactions, and b) yield the necessary information on neutrino reaction products. The event information may vary somewhat with particular experiments, but the basic requirements are tracking, energy measurements, and particle identification. Given currently available detector technology, the most suitable choice of geometry is a sandwich design, with target layers interspersed with tracking devices. The target layers themselves may be either active detector elements (for example, scintillator or Cerenkov counters), or simply passive layers of target material, or a combination of both. Thus, there is a flexibility in the nature of the target material which could be used to "tune" the detector for different experiments at modest costs compared with the total detector construction.

Our study has mainly focused on the size, granularity, and tracking requirements for such a detector at the PSR.

The size of the detector (amount of target material) is primarily determined by counting rate. Cross section measurements will require a few counts/day. The cross sections of interest range from $\sim 10^{-41}$ cm^2 to $\sim 10^{-39}$ cm^2. The incident flux at the PSR is estimated to be $\sim 2 \times 10^5$ ν_μ/cm^2-s (at 50 m without focusing device). This implies

a detector of $\geq$100 tons fiducial volume to obtain a few counts/day at $\sim 10^{-40}$ cm^2. (Note that, with these conditions, we get 0.1/day for ν-e scattering.) We therefore conclude that a large detector of at least $\sim$100 tons will be required to adequately pursue the physics at the proposed facility.

The most stringent requirement on granularity comes from envisioned experiments requiring detection of recoil nucleons from ν-interactions. Detailed studies of such reactions are one of the strongest motivations for building a large neutrino facility that eventually can take advantage of the PSR. For these experiments, it is essential to detect low-energy ($\sim$50 MeV) protons. This requires thin target modules to allow the nucleon to reach the tracking detectors before stopping. The range of a 50-MeV proton is $\sim$2 g/cm^2, so a target thickness of <2 cm (for ρ = 1 g/cm^3) is necessary. Of course, thinner granularity would be preferable but requires more tracking modules. This granularity implies $\sim$400 target and tracking modules to achieve about 100 tons of 1 g/cm^3 target material. It goes without saying that the stringent requirements for fine granularity would be relaxed if the neutrino energy could be increased. Such an increase obviously would also be beneficial for the event rate.

The tracking accuracy that will be required is rather modest compared with state-of-the-art capabilities. The low trigger rate and low multiplicity of events plus multiple scattering of final state particles imply that position resolution of a few millimetersis sufficient to extract meaningful information. It should be noted that very short tracks will fire only one set of tracking modules, and measurement of the angle of such tracks would require two sets of x-y coordinates between layers. In addition to increasing the number of tracking detectors, the physical size of the detector would become significantly larger due to spreading out the modules to obtain sufficient angular resolution. It seems undesirable to incorporate such a capability in the first-generation detector.

One last comment about the detector is that dE/dx capability should be available in the tracking detectors themselves. Because the target modules may or may not yield information, even a crude ($\sim$30%) measurement of dE/dx in the tracking chambers would be very useful.

The last important part of any neutrino detector is the shield. In addition to the main steel shield between the production target and detector,

side shielding is probably necessary. This probably implies that the detector should be placed underground. This also would allow more overhead shielding to be installed than a surface location. If possible, it would be useful to install monitor counters in the steel shield, so that background falloff studies can be undertaken.

The favorable duty-factor of the PSR will improve rejection of cosmic rays, but some further shielding against cosmic rays will probably be needed. The valuable experience of Exp.-31 and forthcoming information from Exp.-225 will help guide these considerations. At present, the best guess is that an active shield close to the walls of the detector house plus a passive shield of steel or lead inside the active shield will provide adequate rejection of cosmic rays. The large size of this active shield means that some care must be taken to prevent dead time problems because of high rates. Crude position resolution (<30 cm) would allow spatial correlation of suspected cosmic ray events in the detector.

The approximate cost has been estimated by comparing the size, number of elements, etc., with existing detectors. We estimate an equipment cost of ~$12 M. This includes the active elements in the shield.

WORKING GROUP ON COSTS AND FACILITIES

L. E. Agnew (Chairman), T. J. Bowles, R. J. Macek,

P. Nemethy, G. J. Stephenson Jr., and R. Werbeck

I. INTRODUCTION

The Committee viewed its assignment as a charge to consider the practicability and feasibility of new facilities that might be proposed, to review their compatibility with existing and other known potential facilities, and to estimate (at an appropriate level of detail) the expected cost of establishing and maintaining them.

II. MOVING TARGET VS. MOVING DETECTOR

Any proposed facility should have the ability to address neutrino oscillations, which implies drawing a variable source-detector distance. Although this is usually achieved by moving the detector, a proposal[1] for an extension of beam line D for a ν_μ disappearance experiment called for use of the LAMPF beam with a fixed detector at the end of a long tunnel that was suitable for a movable target/pion decay volume. This concept appeared to be economically sound because the tunnel for a target system could be much smaller than the tunnel for the detector, and because the LAMPF beam quality is good enough that a relatively small number of small-diameter beam transport elements would be needed.

The use of the Proton Storage Ring (PSR) changes the situation substantially. The phase space of the output beam from the PSR is predicted to be about a factor of 20 larger than the LAMPF output beam. This difference implies a need for a 15-cm quad doublet every 6 m instead of a 10-cm quad doublet every 20-25 m for transport of a straight beam. Beam transport components (magnets, supports, vacuum systems, power supplies, power cables, diagnostics, controls, etc.) will cost approximately $4 M for a 200-m-long tunnel, as compared with approximately $1 M for the earlier version. More-

over, the handling problems involved in changing the length of the beam line in an activated tunnel will be much more severe in the case of increased size and number of components.

However, a movable detector with a total weight of 500-1000 tons means increased costs in other areas, because of a larger-diameter tunnel, heavier footings, more complicated detector structure, etc. The larger tunnel will cost approximately $2 M, instead of $1 M for the earlier version.*

Operating costs (maintenance and power consumption) will be sharply increased for a 200-m beam transport line.

The Committee concluded that a basically stationary target configuration should be adopted; however, provision for varying the length of the decay volume should be maintained. Although a number of factors might point toward this conclusion (for example, simpler target handling, beam line logistics, tunnel activation, etc.), a sufficient argument appears to be that it should be about $2 M cheaper to build, and also cheaper to operate and maintain.

III. TARGET CONSIDERATIONS

Graphite targets for the production of pions are in routine use at LAMPF, using 800-MeV proton beams at currents up to 600 μA. The problems of target survival at high power levels, heat removal from the nearby hardware, radiation-hardened instrumentation, and remote-handling maintenance have largely been solved. This technology can easily be extended to the construction and maintenance of a target cell for the neutrino facility.

The details of the target design can have a substantial effect on the energy spectrum and flux of the pions emerging from the target. Studies of such parameters as target length, target diameter, proton beam profile, target material, etc., should be continued to optimize the neutrino production. One variation in target geometry that was suggested for an in-flight neutrino source is a relatively long target, tilted at a small angle, that is traversed by a proton beam at the same angle in such a way that most of the pion-

*These cost estimates are based on preliminary conceptual designs and past cost experience. It is to be expected that cost estimates based on detailed designs, and that include several years of price escalation plus reasonable contingency funds, will be at least twice as high.

production interactions occur near the surface. A tilted target appears to have some advantages, such as disposal of the pass-through protons (they pose both heat removal and activation problems), slight reduction of the fast neutron flux, and reduced pion energy degradation in the target. The extra cost for a simple bending magnet and power supply system is $100 K.

The target cell should be flexible enough to accommodate future developments such as target sharing by other experiments, storage and focusing devices, and upgraded intensity (more shielding, more cooling, and more remote handling).

IV. DETECTOR CONFIGURATION

It is evident that a second detector could be installed in a tandem position in the tunnel without increasing the primary shielding. A side-by-side dual detector would not be suitable for a movable detector experiment because the costs of the tunnel and primary shielding would be excessive. A fixed-position second detector that utilizes a beam stop source would be cheaper at 90° than 0° because it would need only about two-thirds as much primary shielding. (Our guideline is that 6 by 6 by 9 m of steel is needed at 0°, while only 6 by 6 by 6 m is needed at 90°.) Perhaps a building and the shielding could be obtained for not much more than $1 M at the 90° position.

The 90° position is expected to be more suitable for a "muon bottle"-type of source.

V. MUON STORAGE AND PION FOCUSING DEVICES

Substantial gains in flux (say, factors of 3 to 10) are possible with pion focusing devices, and a muon storage system could provide a unique ν_e source. However, such devices will affect the target assembly geometry and shared beam considerations. The costs of such devices could be very substantial because of the design and development effort required, and also because large magnetic field volumes and radiation hardening will be needed. Cost estimates cannot be made without better definitions; design studies should continue with high priority.

VI. OVERALL CONFIGURATION

A consideration of the siting of a neutrino facility should include the potential needs of other physics programs or research facilities that might compete for the available space in the future. It was the policy of the Neutrino Workshop to acknowledge such possibilities (where known) and to consider (briefly) how they might be compatible with a configuration that fits the needs of a neutrino facility. We found that adequate space is available on the mesa south of the WNR facility to accommodate, with some compromises, the following (see Fig. 1):

a. The neutrino facility with a long detector tunnel, as shown in Figs. 1-4.

b. A possible pulsed mu/pi facility using the neutrino target, or perhaps an upstream thin target (see the Macek Committee report).

c. A potential major new high-current pulsed-neutron facility. Line D could be extended to the west of the proposed neutrino facility. The neutron facility would have a large experimental hall and a number of neutron flight paths. Group P-8 at Los Alamos has made conceptual plans for such a facility.

VII. PSR MODIFICATIONS

The following major PSR modifications, which would enhance the neutrino performance, were mentioned during the Workshop:

a. An increase in the energy.

b. A major increase in the PSR current limit.

c. Alternative spill modes.

These topics, because they require many man-months of study by specialists, are outside the scope of the Workshop and are not considered here. They could be studied by the Laboratory at an appropriate time.

The cost of upgrading the LAMPF/PSR operation from the 100-μA level already committed to the 200-μA level necessary to carry out the proposed neutrino research program is not amenable to a sound estimate. An apparently straightforward way to reach 200 μA would be to double the projected Line D/PSR duty factor on the basis of LAMPF scientific priorities. However,

the system under construction is committed to a design goal of 100 μA, and there are a number of uncertain factors that could require additional effort. These include the H^- source performance, H^- beam acceleration, beam spill in Line D, beam spill in the PSR, etc. Expected beam losses in the PSR are uncertain to a factor of 10 at this time; this is the biggest unknown factor in discussions of the PSR current limit. The ring tunnel is being constructed large enough for future installation (if necessary) of additional transport, more local shielding, and expanded remote handling. Correcting for known shortcomings (for example, a higher duty factor for the kicker magnets) would cost a relatively modest amount--say below $1 M. On the other hand, marginal performance of the LAMPF/PSR system at 100 μA could mean a multimillion dollar investment to reach 200 μA.

In full awareness of the large uncertainties involved, the Committee recommends that a figure of $1 M be assumed for the cost of upgrading to 200 μA. It is recommended that, if at all possible, a firmer figure be developed for the formal proposal to the US Department of Energy.

REFERENCES

1. "A Search for Oscillations Using Muon-Neutrinos at the Los Alamos Meson Physics Facility," LAMPF Proposal 638, T. Dombeck, Spokesman.

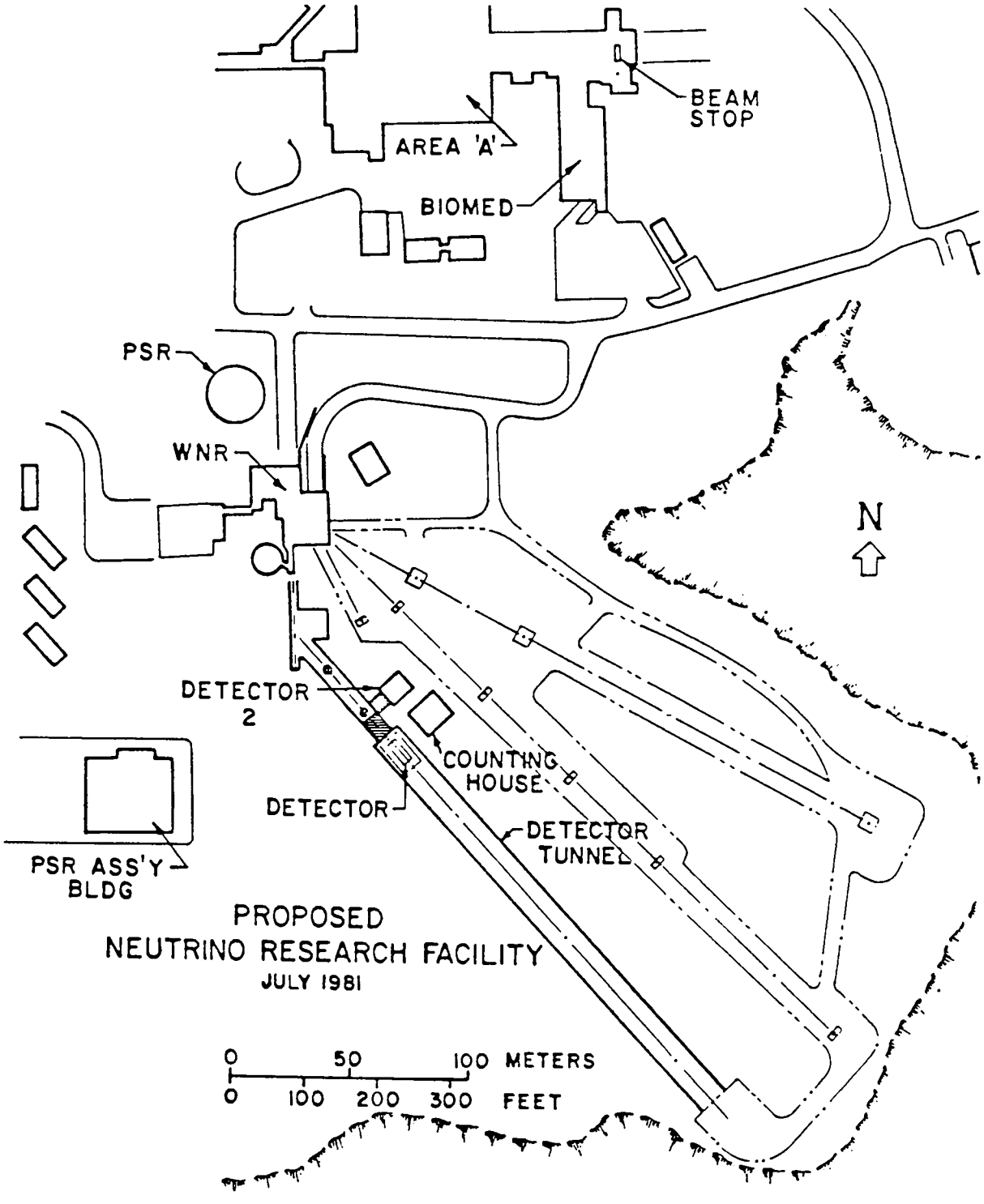

Fig. 1. Plan view of facility discussed in text.

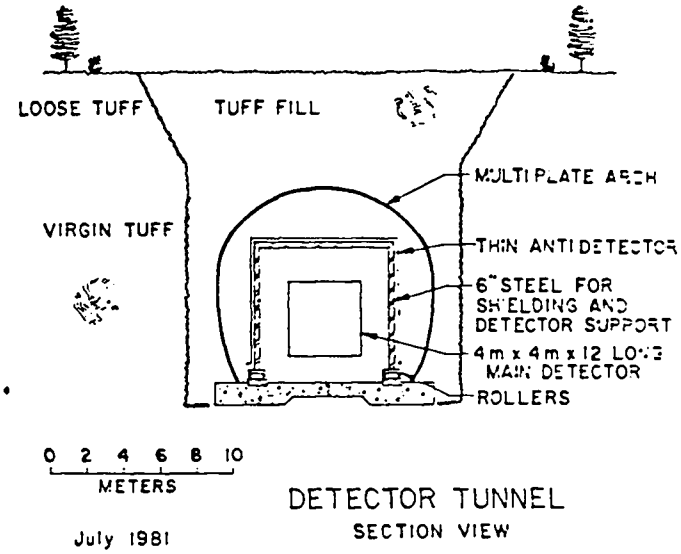

Fig. 2. Detector tunnel discussed in text.

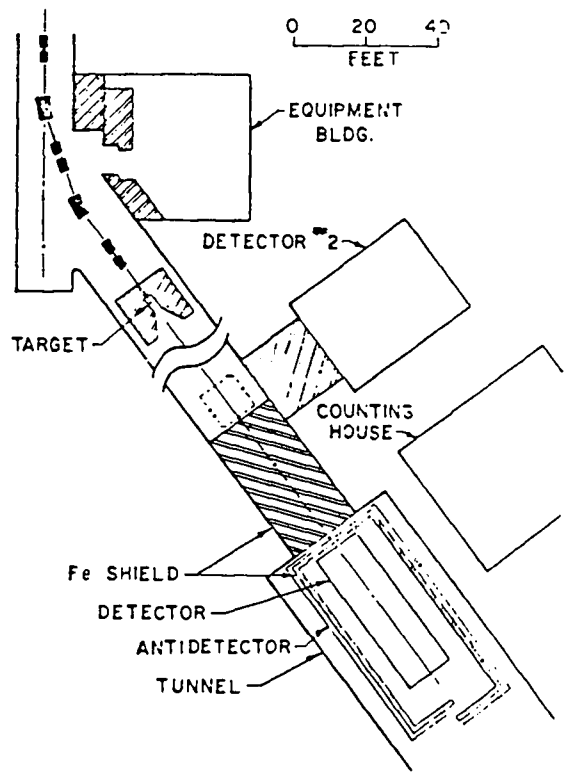

Fig. 3. Expanded plan view.

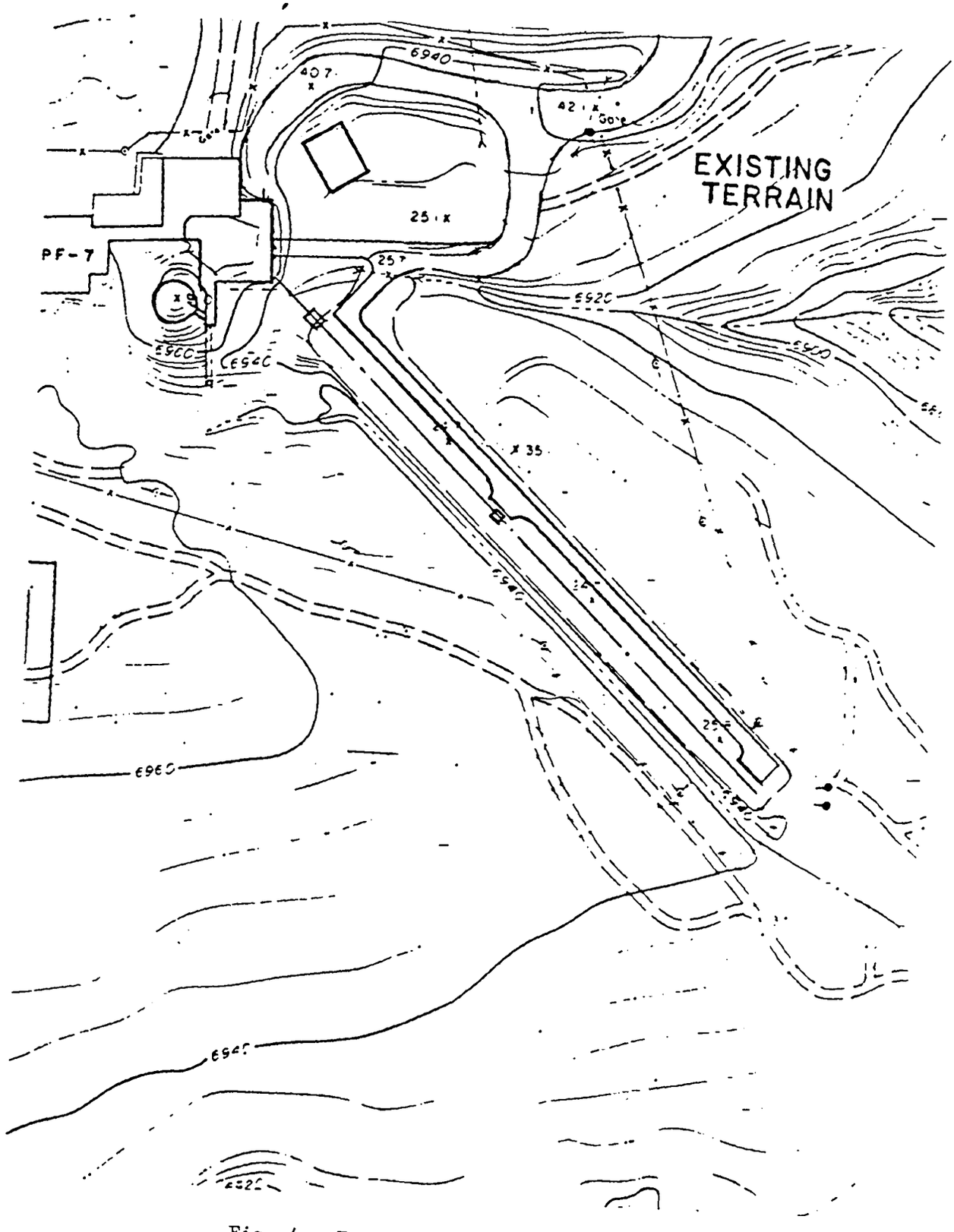

Fig. 4. Topography of facility site.

WORKING GROUP ON PULSED MU/PI BEAMS AND OTHER USES

R. J. Macek (Chairman), L. Agnew, T. Bowles, D. Bryman, T. Goldman,

R. Heffner, R. Redwine, G. Sanders, and R. Werbeck

I. INTRODUCTION

This working group was formed to examine other basic research facilities that might share primary beam with a future neutrino facility.

We initially considered four main facilities:

1. Pulsed mu/pi beams.
2. Pulsed external proton beams.
3. Fast-pulsed neutron beams.
4. A second pulsed spallation neutron source.

The WNR spallation neutron source exists and will be upgraded as part of the PSR project; it was not a topic for further discussion. Fast neutron and external proton beams are of interest for studies of the N-N interactions and for use as nuclear physics probes. The demand for fast neutron and external proton beams is expected to be relatively infrequent and can be adequately met at WNR or in occasional setups in Line D. This left pulsed mu/pi beams and a second spallation neutron source as the chief topics for further study by this working group.

II. PULSED MU/PI BEAMS

A. Scientific Merit

An informal working group, chaired by R. Heffner, has been meeting since January 1981 to study the scientific merit and technical feasibility for a pulsed muon facility at PSR. A report from this group was summarized by R. Heffner and is included as the Appendix of this report. Table II of the Heffner report is a good summary of the muon experiments that particularly benefit from the unique features of a pulsed muon beam. These experiments fall into several broad classes:

1. Those that study delayed processes where beam-associated backgrounds can be reduced by a prompt timing cut.
2. Time differential μSR experiments where all muons arrive at the target within a few nanoseconds, thereby eliminating the need for pile-up rejection.
3. Experiments carried out in intrinsically pulsed environments such as ones requiring laser pumping of muonic atoms.
4. Measurements of the muonium hyperfine structure interval using the line narrowing techniques available with pulsed beams.

For certain experiments it is possible to quantify the advantages of a pulsed muon beam at PSR in comparison with beams available elsewhere. For time differential μSR, the pulsed beam technique will allow data rates 10 times that achievable with a dc machine such as SIN.

It is probably possible to pulse low-momentum beams at the LAMPF Stopped Muon Channel (SMC) and gain some advantage as compared with not pulsing; however, at 100 MA, the PSR based muon beam would have several times the rate advantage for the same acceptance compared with pulsing the SMC. Furthermore, the extinction factor (ratio of flux for beam-off period to beam-on period) is many orders of magnitude better at PSR. The (μ,e) conversion experiments need an extinction factor of 10^{-8} or better whereas a pulsed SMC might be as good as 10^{-3}.

For measurements of the muonium hyperfine structure interval, V. Hughes estimates a factor of 3-4 better result because of line narrowing with pulsed beams. In addition, the PSR muon beam would allow a factor of 5-20 higher data rate compared with a pulsed SMC.

This working group agrees with the conclusion of the Heffner report. There is a broad spectrum of important science ranging from studies of fundamental interactions to nuclear physics and material science that would be substantially improved by using the pulsed muon beams potentially available at PSR. Furthermore, this facility could be more advantageous and more versatile than any existing pulsed muon beam such as those at KEK or the Brookhaven AGS.

B. Facility Requirements/Criteria

The following list of requirements and criteria was developed for the design of a general purpose pulsed muon channel:

1. Provide both "decay" and "surface" stopping muon beams with $\Delta R \simeq 1$ g/cm. This implies $\lesssim$100 MeV/c muons.
2. Use both short and long burst mode primary beams.
3. A large acceptance, high flux design with flexible phase-space tailoring and output tuning capabilities.
   a. $\sim 10^7$ μ^-/s at 100 μA.
   b. $>10^5$ μ^+/s into a 1-in. spot in the short burst mode, primarily for μSR experiments.
4. High polarization. Include a spin precessor capable of at least 90° rotation of muon spin.
5. Isochronous to ~2 ns.
6. Good purity, e/μ <1%.

A channel meeting these requirements would benefit all the experiments mentioned in the Heffner report. It was generally agreed that such a channel was technically feasible using existing technology.

C. Beam Sharing and Possible Site for a Pulsed Muon Facility

Whereas a pulsed muon facility has considerable merit, it may not justify sole use of the PSR beam for large amounts of running time. For this reason the working group gave extra consideration to means of simultaneously sharing the beam with other users. The following three possibilities emerged as viable alternatives:

1. Sharing the WNR I/(II) target.
2. Sharing a target or target location with a neutrino facility.
3. Use of a thin target (but thick enough for a muon facility) upstream of the neutron or neutrino facilities.

The most viable or most compatible alternative is not clear at this time; more work is needed to evaluate the costs and other impacts for each alternative. G. Sanders and R. Werbeck agreed to explore with the WNR management the feasibility of sharing the WNR target. Their evaluation will not be available in time for this report. It is obvious that sharing the WNR target will not be easy; any practical scheme will likely impose new constraints on the muon channel design.

The viability of sharing a target with a future neutrino facility depends upon characteristics of the target configuration that are still uncertain. For example, if the target must move for the oscillation experiments, then

compatibility is much more restricted. Even for a fixed target the access may be blocked by a focusing device or a future pion/muon bottle.

A thin target upstream of a neutrino target will increase the primary beam phase space and may compromise the spot size at the neutrino target. It may also produce unacceptable backgrounds from secondaries produced upstream. These considerations require further detailed work for proper evaluation; they may or may not be deciding factors.

A thin target upstream of WNR will likely not compromise the beam spot for thermal neutron work; however, spatial constraints appear to make it impractical. This need not be a constraint for a future spallation neutron source located farther out on the mesa.

III. A SECOND SPALLATION NEUTRON SOURCE

From R. Silver we heard a proposal for a major upgrade of the neutron facilities for condensed matter physics. He proposes a new, higher intensity facility farther out on the mesa. It would be capable of handling 400 μA, which implies a future upgrade of PSR and more beam from LAMPF. It would have a horizontal target with a beam entering the target in a horizontal plane. It could also have a forward, fast neutron port with a long flight path.

At one time they looked carefully at sharing such a target with neutrino users but concluded that they were not sufficiently compatible. Each would be better off with separate targets even though they would each lose a factor of two in integrated beam intensity. Their losses through sharing would be significantly greater.

There is a potential space conflict with a long neutrino line. One resolution might be to separate them in the vertical dimension by having the neutron facility set on the surface while the neutrino line is well beneath the surface.

IV. CONCLUSIONS AND RECOMMENDATIONS

This group recommends that the neutrino facility proposal leave room for the possible addition of a future pulsed muon channel. There is considerable scientific interest in and merit to a pulsed muon facility at PSR. This working group believes that it is a highly desirable part of an experimental

area that fully exploits the unique capabilities of PSR. It becomes highly attractive if a way can be found to share the beam simultaneously with another facility.

APPENDIX A

Summary of the January 1981 PSR-Muon Channel Working Group Discussions

R. H. Heffner

I. INTRODUCTION

A working group was formed in late January 1981 to study the scientific justification and technical feasibility for a pulsed muon facility at the Los Alamos Proton Storage Ring (PSR). The group has met 4-5 times to date. The members of the working group have been T. Bowles (P-3), J. Donahue (MP-7), M. Gladisch (Yale/Heidelberg), R. Heffner (MP-3, Chairman), A. Jason (AT-3), W. Johnson (P-3), K. Krane (Oregon State), R. Macek (MP-13), and G. Sanders (MP-13). In addition, A. Sachs from Columbia University was invited to address the group regarding the uses and status of the BNL pulsed muon channel.

The agenda for the working group was to first examine the scientific justification for a pulsed muon facility and then, if the science looked promising, address the technological questions of channel design, costs, and compatibility with other PSR scientific endeavors, most notably neutrino and neutron physics. To date the group has formulated a preliminary list of experiments which would be suitable for such a facility and has just begun to examine the technical questions mentioned above. This report summarizes the discussions of the working group for the benefit of the members of the Neutrino Workshop held at Los Alamos, June 8-12, 1981.

II. PSR CHARACTERISTICS

Relevant PSR parameters for the two modes of operation currently envisioned are as as listed in Table I, below:

III. SCIENTIFIC JUSTIFICATION FOR A PULSED MUON FACILITY

The emphasis of the working group thus far has been on determining the scope of experiments which could be substantially improved by use of a muon beam pulsed with the characteristics of the PSR (Table I). (A possible

interest in pulsed pion beams was noted, but not yet addressed.) Table II is a compilation of the experiments that were found to be particularly suitable to a PSR-muon facility. Such experiments generally fall into several broad categories of which a few are listed here: 1) those studies that look for delayed processes wherein background from beam-associated reactions has died away (μ capture and fission, μ → e conversion, etc.), 2) experiments carried out using intrinsically pulsed environments such as radio frequency or laser pumping of muonic atoms, 3) time differential μSR experiments wherein all muons arrive at the target within a few nanoseconds, thus eliminating the need for pile-up rejection (and yielding a data rate 10 times that achievable with a dc machine such as SIN), 4) muonium hyperfine field studies that use the pulsed nature of the muon beam to significantly reduce line widths and hence increase precision.

Two points regarding this table should be emphasized: 1) It is immediately apparent from the breadth of applications that nearly all combinations of muon beams (μ^+, μ^-, decay and surface beams) and PSR modes (long and short) should be planned for. 2) The list is by no means intended to be exhaustive; rather, it represents the interests of several current muon users at LAMPF. Nevertheless, it was the consensus of the working group that even this preliminary spectrum of experiments was stimulating enough to proceed with a serious design for a PSR-muon channel.

IV. MUON BEAM CHARACTERISTICS

A. Intensity Achievable at the PSR

For orientation one may imagine moving the LAMPF SMC and A-2 target to the PSR. Rough estimates of the total μ^+ intensities in a large spot for the short pulse mode are as follows:

128 MeV/c (decay beam) : 6×10^5/s
80 MeV/c (decay beam) : 3×10^5/s
28 MeV/c (surface beam) : 1×10^6/s.

The estimates for the long pulse mode are about 10 times larger, and the μ^- intensities for decay beams are about 20-25% of the μ^+ intensities. For comparison the SIN μE1 channel produces about 10 times more μ^+/proton at 128 MeV/c than the LAMPF-SMC channel. A major area of future study must

involve a realistic estimate of muon fluxes attainable with a channel tailored to the PSR. Even so, a factor of 10 improvement over the above numbers is a reasonable expectation.

B. Isochronicity in the Short Pulse Mode

An important unanswered question concerns the degree to which the 1-ns-proton burst width is preserved in the muon pulse width. A degradation of much more than a factor of three would be undesirable for many of the short pulse mode experiments listed in Table II.

C. Other

Most muon experiments require a beam of high luminosity, high polarization, and high stopping density, as well as low contamination from pions and/or electrons. This again must be a subject for future study.

V. COMPARISON WITH OTHER FACILITIES

A. KEK Booster

From Table III one would expect a PSR-muon channel to produce equal or greater average muon intensities than the KEK facility with a comparable duty factor. The real advantage of the PSR would appear to be the capability of producing extremely short pulses ($\sim$1 ns).

B. Brookhaven AGS

The AGS has two possible operating modes: 1) a uniform 1-s-proton beam burst followed by a 1.5-s wait for acceleration (40% macroscopic duty factor), and 2) a single pulse mode of $\simeq 10^{12}$ protons arriving within $\simeq$ 5 ns, followed by a 1.5-2.5-s wait for acceleration ($\sim 2 \times 10^{-9}$ duty factor). A muon channel consisting of components from Nevis and SREL is planned to be operational at BNL in the fall of 1982. The calculated muon stopping rate is about 2×10^{4}/s in a 2- x 2-cm spot for the mode (1) above. The extremely short duty factor of $\simeq 10^{-9}$ (compared with $\simeq 10^{-6}$ for the PSR and the KEK facilities) probably makes the AGS short pulse mode impractical.

C. Chopping in Secondary Beam Lines at LAMPF

Chopping in the H^+ beam at up to 10% of the LAMPF duty factor is possible, though not particularly desirable since all LAMPF beams would be affected. A more palatable scheme would be to chop the secondary (muon or pion) beam itself using either electrostatic plates or time-varying magnetic fields. The plates would be best for frequencies ≃50 MHz while the magnet would be best for ≃1 MHz. The 1-10 MHz range is more suitable for rare-muon decay mode experiments, for example, than is the PSR because of the small PSR duty factor. (For such studies one wants a beam on-off interval which is better matched to the muon lifetime, that is, a few microseconds.) The 50 MHz chopping would be useful for stroboscopic μSR studies.

VI. SUMMARY

There appears to be a broad spectrum of important science (ranging from studies of fundamental interactions to nuclear physics and materials science) that would be substantially benefited by using the pulsed muon and pion beams potentially available at the PSR. Furthermore, the PSR facility looks more favorable and versatile than either the Brookhaven AGS or the KEK facilities, especially in its ability to produce extremely short pulses (∿1 nsec) at a reasonable duty factor (∿10^{-6}). This capability would be unmatched in the world. Therefore, the major tasks that lie ahead are as follows:

1. An accurate assessment of the performance characteristics which might be expected for a PSR muon/pion channel,
2. A further look at the scope of the scientific program which one envisions with emphasis on extending the program to pion reactions and making a semiquantitative comparison of the experimental results if carried out at the SMC or at the PSR (that is, how much does the PSR improve things?),
3. A hard look at the compatibility of the various possible facilities and/or uses of the PSR, nominally, neutron scattering for both materials science and nuclear physics, neutrino physics, and muon/pion physics.

IV. CONCLUSIONS

The workshop has identified several fundamental issues in neutrino physics that can only be resolved with a medium-energy neutrino beam at low duty cycle. Among the experiments considered are the following: neutrino oscillations, $\nu_\mu e$ and $\nu_e e$ scattering, $\nu_\mu p$ and $\nu_e p$ scattering, charged and neutral current reactions on the deuteron, neutrino-nucleus coherent scattering, and neutrino-nucleus inelastic scattering through both neutral and charged currents.

We recommend that planning of a neutrino facility at Los Alamos should proceed, and that a proposal should be prepared detailing the various issues raised at this workshop and documented in this report. In addition, special attention should be directed in the future to extended studies of a muon bottle, new detector technology, and the possibility and desirability of increasing the neutrino energy.

A-TABLE I

	Proton Pulse Width	Frequency	Av Current	Protons/s
Short mode	1 ms	720 Hz	12 μA	7.5×10^{13}
Long mode	270 ns	12 Hz	100 μA	6.25×10^{14}

A–TABLE II

EXPERIMENTS	MUON POLARITY	BEAMS DECAY/SURFACE	PSR PULSE MODE
I. Muon Capture			
1. Muon-induced fission	Negative	Decay or Cloud	Short
2. Specific states in final nuclei a. test PCAC b. nuclear moments	Negative	Decay or Cloud	Short
3. Parity mixing in atomic cascade	Negative	Decay or Cloud	Short
4. Capture lifetimes in light elements (hydrogen)	Negative	Decay or Cloud	Long
5. Muonic Helium a. h.f.s. and magnetic moment of μ^-	Negative	Decay	Long
6. Optical transitions a. Lamb shift in μ^-p, $\mu^- {}^3He$ and $\mu^- {}^4He$	Negative	Decay or Cloud	Short
b. h.f.s. in μ^-p	Negative	Decay or Cloud	Short
II. Muon Spin Rotation			
1. Correlation times in phase transitions	Either (mostly positive)	Surface or Decay	Short
2. Muon/hydrogen diffusion in metals	Positive	Surface or Decay	Short
3. Impurity centers in semiconductors, insulators	Positive	Surface or Decay	Short
4. Muonium chemistry a. reaction rates	Positive	Surface	Short
b. free radicals			
III. Muonium h.f.s. Studies	Positive	Surface	Long
IV. $\mu^- + Z \rightarrow e^- + Z$	Negative	Decay or Cloud	Long
V. $\mu^+e^- \rightarrow \mu^-e^+$ in vacuum	Positive	Surface	Long
VI. Muon Lifetime	Positive Negative	Surface or Decay	Long
VII. μ^+ Magnetic Moment	Positive	Surface or Decay	Short

A-TABLE III

		KEK	PSR	
			Short	Long
1.	Proton Beam			
	Energy	500	800	800 (MeV)
	Frequency	20	720	12 (Hz)
	Width	50	1	270 (ns)
	Proton/pulse	3×10^{11}	1×10^{11}	5.2×10^{13}
2.	Muon Beam			
	A Intensity	3×10^{6}	To be determined	
	μ^+/Pulse	1.5×10^{5}	To be determined	

APPENDIX B

INTERMEDIATE-ENERGY ELASTIC NEUTRINO SCATTERING FROM NUCLEI

by

T. W. Donnelly

ABSTRACT

Elastic scattering of neutrinos and anti-neutrinos from nuclei via the neutral current weak interaction is studied at intermediate neutrino energies (a few hundred MeV). The angle and energy-dependences of the cross sections are explored for a selection of target nuclei (n, ^{1}H, ^{2}H, ^{4}He, ^{12}C, ^{16}O, ^{27}Al, ^{40}Ca and ^{56}Fe) and the sensitivity of the results to variations of the gauge theory couplings away from the standard model is investigated.

I. Introduction and Summary of Formalism

In the present work the elastic scattering of neutrinos and anti-neutrinos from nuclei is studied at intermediate neutrino energies (a few hundred MeV) as would be available, for example, at the pion decay-in-flight neutrino facility proposed for LAMPF[1]. The formalism for such calculations has been presented in a previous general study of neutral current effects in nuclei[2], which in turn was built upon earlier work on the neutral current weak interaction with nuclei[3-5]. In the present paper only the essence of the development of the

necessary formalism is given; in a subsequent paper details of this development will be expanded upon[6].

The general differential cross section for (elastic or inelastic) neutral current neutrino and anti-neutrino scattering, inducing a nuclear transition from state $|J;TM_T>$ to state $|J';T'M_T>$ was given in Ref. 2 (Eq. (3.26)):

$$\left.\frac{d\sigma}{dq^2}\right|_{\substack{\nu\nu' \\ \bar{\nu}\bar{\nu}'}} (J;TM_T \to J';T'M_T) = 2(G\kappa)^2 \frac{\nu'}{\nu}\cos^2\frac{\theta}{2}$$

$$\times \frac{1}{2J+1}\left\{\sum_{\mathcal{J}\geq 0}\left|\sum_{\mathcal{T}=0,1}\begin{pmatrix} T' & \mathcal{T} & T \\ -M_T & 0 & M_T\end{pmatrix}<J';T'\|\hat{\mathcal{M}}_{\mathcal{J};\mathcal{T}}(q)\|J;T> + \frac{\omega}{q}\hat{\mathcal{L}}_{\mathcal{J};\mathcal{T}}(q)\|J;T>\right|^2\right.$$

$$+\sum_{\mathcal{J}\geq 1}\left[\left(\frac{q_\mu^2}{2q^2}+\tan^2\frac{\theta}{2}\right)\left(\left|\sum_{\mathcal{T}=0,1}\begin{pmatrix} T' & \mathcal{T} & T \\ -M_T & 0 & M_T\end{pmatrix}<J';T'\|\hat{\mathcal{T}}^{el}_{\mathcal{J};\mathcal{T}}(q)\|J;T>\right|^2\right.\right.$$

$$\left.\left.+\left|\sum_{\mathcal{T}=0,1}\begin{pmatrix} T' & \mathcal{T} & T \\ -M_T & 0 & M_T\end{pmatrix}<J';T'\|\hat{\mathcal{T}}^{mag}_{\mathcal{J};\mathcal{T}}(q)\|J;T>\right|^2\right)\right.$$

$$\left.\mp 2\tan\frac{\theta}{2}\left(\frac{q_\mu^2}{q^2}+\tan^2\frac{\theta}{2}\right)^{1/2}\sum_{\mathcal{T},\mathcal{T}'=0,1}\begin{pmatrix} T' & \mathcal{T} & T \\ -M_T & 0 & M_T\end{pmatrix}\begin{pmatrix} T' & \mathcal{T}' & T \\ -M_T & 0 & M_T\end{pmatrix}\right.$$

$$\left.\times \mathcal{R}e<J';T'\|\hat{\mathcal{T}}^{el}_{\mathcal{J};\mathcal{T}}(q)\|J;T><J';T'\|\hat{\mathcal{T}}^{mag}_{\mathcal{J};\mathcal{T}'}(q)\|J;T>^*\right]\right\}. \qquad (1)$$

Here the incident neutrino (or anti-neutrino) energy is ν, the scattered neutrino (or anti-neutrino) energy is ν', the energy transfer (from neutrinos to the nucleus) is $\omega = \nu - \nu'$ and the neutrino scattering angle is θ. From these the three-momentum transfer q and four-momentum transfer q_μ can be determined ($q_\mu^2 = q^2 - \omega^2$). The universal weak interaction coupling constant is G and κ is an overall gauge coupling ($\kappa = 1$ in the standard model = W-S-GIM model, see Ref. 2). We shall return to the nuclear multipole operators shortly.

The nuclear weak neutral current operator may be expanded into four terms:

$$\hat{\mathcal{J}}_\mu = \beta_V^{(0)} (\hat{J}_\mu)_{00} + \beta_A^{(0)} (\hat{J}_\mu^5)_{00} + \beta_V^{(1)} (\hat{J}_\mu)_{10} + \beta_A^{(1)} (\hat{J}_\mu^5)_{10} \ , \tag{2}$$

where the terms are respectively, isoscalar vector current, isoscalar axial-vector current, isovector vector current and isovector axial-vector current (see Ref. 2, Eq. (3.7)). Here the caret indicates a second-quantized operator operating in the nuclear space and the "5" is used to denote axial-vector quantities (from the extra γ_5 in the currents, see Eq. (7) below). The gauge theory couplings $\beta_V^{(\mathcal{T})}$ and $\beta_A^{(\mathcal{T})}$, $\mathcal{T}=0,1$ may be rewritten in terms of the couplings $\alpha_V^{(\mathcal{T})}$ and $\alpha_A^{(\mathcal{T})}$, $\mathcal{T}=0,1$ (see Table 2.1 in Ref. 2):

$$\beta_V^{(\mathcal{T})} = \alpha_V^{(\mathcal{T})} - \alpha_{em} \quad , \ \mathcal{T} = 0,1$$

$$\beta_A^{(\mathcal{T})} = \alpha_A^{(\mathcal{T})} \tag{3}$$

For the standard model one has $\alpha_{em} = 2\sin^2\theta_W = .46$ and

$\alpha_V^{(0)} = \alpha_A^{(0)} = 0$, $\alpha_V^{(1)} = \alpha_A^{(1)} = 1$, thus

$$\beta_V^{(0)} = -.46, \ \beta_A^{(0)} = 0, \ \beta_V^{(1)} = .54, \ \beta_A^{(1)} = 1 \ . \tag{4}$$

Multipole projections of the nuclear current operators are made in the standard manner (see Refs. 2 and 7, for example) resulting in vector and axial-vector multipole operators

$$\hat{M}_{J M_J; \mathcal{T} M_\mathcal{T}}(q) \text{ and } \hat{M}^5_{J M_J; \mathcal{T} M_\mathcal{T}}(q)$$

$$\hat{L}_{J M_J; \mathcal{T} M_\mathcal{T}}(q) \text{ and } \hat{L}^5_{J M_J; \mathcal{T} M_\mathcal{T}}(q)$$

$$\hat{T}^{el}_{J M_J; \mathcal{T} M_\mathcal{T}}(q) \text{ and } \hat{T}^{el5}_{J M_J; \mathcal{T} M_\mathcal{T}}(q)$$

$$\hat{T}^{mag}_{J M_J; \mathcal{T} M_\mathcal{T}}(q) \text{ and } \hat{T}^{mag5}_{J M_J; \mathcal{T} M_\mathcal{T}}(q) \tag{5a}$$

The precise definitions are given in Ref. 2, Eqs. (3.10) and (3.11). The combined V-A multipole operators are then given by

$$\hat{\mathcal{M}}_{J M_J; \mathcal{T} M_\mathcal{T}}(q) = \beta_V^{(\mathcal{T})} \hat{M}_{J M_J; \mathcal{T} M_\mathcal{T}}(q) + \beta_A^{(\mathcal{T})} \hat{M}^5_{J M_J; \mathcal{T} M_\mathcal{T}}(q)$$

$$\hat{\mathcal{L}}_{J M_J; \mathcal{T} M_\mathcal{T}}(q) = \beta_V^{(\mathcal{T})} \hat{L}_{J M_J; \mathcal{T} M_\mathcal{T}}(q) + \beta_A^{(\mathcal{T})} \hat{L}^5_{J M_J; \mathcal{T} M_\mathcal{T}}(q)$$

$$\hat{\mathcal{T}}^{el}_{J M_J; \mathcal{T} M_\mathcal{T}}(q) = \beta_V^{(\mathcal{T})} \hat{T}^{el}_{J M_J; \mathcal{T} M_\mathcal{T}}(q) + \beta_A^{(\mathcal{T})} \hat{T}^{el5}_{J M_J; \mathcal{T} M_\mathcal{T}}(q)$$

$$\hat{\mathcal{J}}^{\text{mag}}_{\mathcal{J}\mathcal{M}_\mathcal{J};\mathcal{J}\mathcal{M}_\mathcal{J}}(q) = \beta_V^{(\mathcal{J})} \hat{T}^{\text{mag}}_{\mathcal{J}\mathcal{M}_\mathcal{J};\mathcal{J}\mathcal{M}_\mathcal{J}}(q) + \beta_A^{(\mathcal{J})} \hat{T}^{\text{mag}5}_{\mathcal{J}\mathcal{M}_\mathcal{J};\mathcal{J}\mathcal{M}_\mathcal{J}}(q) \quad . \tag{5b}$$

As discussed in Ref. 5, for elastic scattering using the parity and time-reversal properties of the multipole operators, only the following may have non-zero matrix elements:

$$\begin{cases} \hat{M}_\mathcal{J} & \text{for even } \mathcal{J} \\ \hat{T}^{\text{mag}}_\mathcal{J}, \ \hat{L}^5_\mathcal{J} \text{ and } \hat{T}^{\text{el}5}_\mathcal{J} & \text{for odd } \mathcal{J}. \end{cases} \tag{6}$$

At this point, given specific descriptions of the nuclear states involved, what remains is to compute the matrix elements of the surviving multipole operators to obtain the cross section in Eq. (1).

For the case of a single nucleon we have in general, using Lorentz covariance, conservation of parity, time-reversal invariance and isospin invariance[2]

$$\begin{aligned} &\langle \vec{k}'\lambda'; \tfrac{1}{2}m_t' | (J_\mu(0))_{\mathcal{J}\mathcal{M}_\mathcal{J}} | \vec{k}\lambda; \tfrac{1}{2}m_t \rangle \\ &= i\bar{u}(\vec{k}'\lambda') [F_1^{(\mathcal{J})} \gamma_\mu + F_2^{(\mathcal{J})} \sigma_{\mu\nu} q_\nu + iF_S^{(\mathcal{J})} q_\mu] u(\vec{k}\lambda) \\ &\times \langle \tfrac{1}{2}m_t' | I_\mathcal{J}^{\mathcal{M}_\mathcal{J}} | \tfrac{1}{2}m_t \rangle \\ &\langle \vec{k}'\lambda'; \tfrac{1}{2}m_t' | (J_\mu^5(0))_{\mathcal{J}\mathcal{M}_\mathcal{J}} | \vec{k}\lambda; \tfrac{1}{2}m_t \rangle \\ &= i\bar{u}(\vec{k}'\lambda') [F_A^{(\mathcal{J})} \gamma_5\gamma_\mu - iF_P^{(\mathcal{J})} \gamma_5 q_\mu - F_T^{(\mathcal{J})} \gamma_5 \sigma_{\mu\nu} q_\nu] u(\vec{k}\lambda) \\ &\times \langle \tfrac{1}{2}m_t' | I_\mathcal{J}^{\mathcal{M}_\mathcal{J}} | \tfrac{1}{2}m_t \rangle \ , \end{aligned} \tag{7}$$

where the states are labelled by three-momentum $\vec{k}(\vec{k}')$, helicity $\lambda(\lambda')$ and isospin $\frac{1}{2}m_t(\frac{1}{2}m_t')$. The momentum transfer is given by $q_\mu = k_\mu - k'_\mu$. The isospin dependence of the single-nucleon currents is contained in

$$I^{M_J}_{J} \equiv \frac{1}{2} \times \begin{cases} 1 & J = 0,\ M_J = 0 \\ \tau_0 = \tau_3 & J = 1,\ M_J = 0 \\ \tau_{\pm 1} = \mp \frac{1}{\sqrt{2}}(\tau_1 \pm i\tau_2) & J = 1,\ M_J = \pm 1, \end{cases} \tag{8}$$

where we only require the $M_J = 0$ pieces for descriptions of neutral current neutrino scattering. We shall assume that there are no second-class currents, in which case $F_S^{(J)} = F_T^{(J)} = 0$. In addition for scattering of massless neutrinos the induced pseudoscalar contribution can be shown to vanish; thus we may ignore the $F_P^{(J)}$ terms and the effective dependence will be on $F_1^{(J)}\gamma_\mu + F_2^{(J)}\sigma_{\mu\nu}q_\nu$ for the vector current and on $F_A^{(J)}\gamma_5\gamma_\mu$ for the axial-vector current. For the single-nucleon form factors we take

$$\begin{aligned} F_1^{(J)}(q_\mu^2) &= F_1^{(J)}(0) f_V(q_\mu^2) \\ F_2^{(J)}(q_\mu^2) &= F_2^{(J)}(0) f_V(q_\mu^2) \\ F_A^{(J)}(q_\mu^2) &= F_A^{(J)}(0) f_A(q_\mu^2), \qquad J = 0 \text{ and } 1, \end{aligned} \tag{9a}$$

with $F_1^{(0)}(0) = F_1^{(1)}(0) = 1$

$$F_1^{(0)}(0) + 2M_N F_2^{(0)}(0) \equiv \mu^{(0)}(0) = .8798 \quad \text{(isocalar magnetic moment)}$$

$$F_1^{(1)}(0) + 2M_N F_2^{(1)}(0) = \mu^{(1)}(0) = 4.706 \quad \text{(isovector magnetic moment)}$$

$$F_A^{(1)}(0) = -1.23 \quad \text{(from n } \beta\text{-decay)} \tag{9b}$$

$$F_A^{(0)}(0) = \frac{3}{5} F_A^{(1)}(0) \quad \text{(static quark model)} \ ,$$

where M_N is the nucleon mass,

and dipole parameterizations of the form factors:

$$f_V(q_\mu^2) = [1 + q_\mu^2/m_V^2]^{-2}$$

$$f_A(q_\mu^2) = [1 + q_\mu^2/m_A^2]^{-2} \ , \tag{9c}$$

with $m_V = 855$ MeV and $m_A = 890$ MeV.

It is straightforward to proceed from these free single-nucleon matrix elements to a non-relativistic reduction in a single-particle basis more suited to nuclear calculations involving quantum numbers $\alpha \equiv \{n(\ell\frac{1}{2})jm_j;\frac{1}{2}m_t\}$. The relevant expressions and tables of all required reduced matrix elements are given in Ref. 7 (see also Eqs. (3.31) and (3.32) in Ref. 2).

The remaining step in calculating the matrix elements required in Eq. (1) involves assuming that the nuclear current operators may be taken to be one-body operators for the range of energy-momentum of interest. This is done in the present work:

$$\hat{T}_{J M_J;T M_T}(q) = \sum_{\alpha\alpha'} \langle \alpha' | T_{J M_J;T M_T}(q) | \alpha \rangle a_{\alpha'}^\dagger a_\alpha \ , \tag{10}$$

where $\hat{T}$ is any one of the multipole operators, $\langle \alpha' | T_{J M_J;T M_T}(q) | \alpha \rangle$ are single-particle matrix elements labelled with single-particle

sets of quantum numbers α,α' and $a^\dagger_{\alpha'}$, and a_α are creation and destruction operators respectively. In writing Eq. (10) we have ignored, for example, explicit two-body meson exchange current effects. Taking nuclear matrix elements between states s' (with J', T') and s (with J, T) we obtain

$$\langle J';T'\|\hat{T}_{\mathcal{J};\mathcal{T}}(q)\|J;T\rangle = \sum_{aa'} \langle a'\|T_{\mathcal{J};\mathcal{T}}(q)\|a\rangle \psi^{(s's)}_{\mathcal{J};\mathcal{T}}(a'a) \ , \qquad (11)$$

where the symbols $\|\ \|$ denoté matrix elements reduced in angular momentum and isospin, $\langle a'\|T_{\mathcal{J};\mathcal{T}}(q)\|a\rangle$ are doubly-reduced single-particle matrix elements (obtained using the tables in Ref. 7) labelled with single-particle sets of quantum numbers $a \equiv \{n(\ell\tfrac{1}{2})j;\tfrac{1}{2}\}$ and where the expansion coefficients are one-body density matrix elements given by

$$\psi^{(s's)}_{\mathcal{J};\mathcal{T}}(a'a) = \langle J';T'\|\hat{\xi}^\dagger_{a'a}(\mathcal{J};\mathcal{T})\|J;T\rangle/\sqrt{(2\mathcal{J}+1)(2\mathcal{T}+1)} \ , \qquad (12)$$

where $\xi^\dagger_{a'a}(\mathcal{J}M_{\mathcal{J}};\mathcal{T}M_{\mathcal{T}})$ is a tensor product of $a^\dagger_{n'(\ell'\frac{1}{2})j'm'_j;\frac{1}{2}m'_t}$ and $(-)^{j-m_j}(-)^{(1/2)-m_t}a_{n(\ell\frac{1}{2})j,-m_j;\frac{1}{2},-m_t}$. The only approximation here is in assuming that the multipole operators are one-body operators as long as the expansions run over complete sets of single-particle wave functions.

Specifically for the present problem of elastic neutrino scattering we have s'(J',T') = s(J,T) and for these ground states shall assume that the nucleons are occupying all single-particle levels up to the Fermi surface and occupy no levels above this; that is, we shall take the ground states to be the most natural uncorrelated shell model configurations[†]:

[†]For the ^{2}H case, a $^3S_1 + {}^3D_1$ ground state is also considered (see below).

also. Of course for elastic scattering from nuclei heavier than the proton detection of the nuclear recoil should provide a distinctive signal as the only coherent effect is in the elastic event.

Acknowledgements

This work was stimulated by the need for elastic neutrino scattering cross sections identified at the Los Alamos Neutrino Workshop in June, 1981. The author wishes to thank the organizers, F. Boehm and G. Stephenson, for the invitation to attend. Early development of the necessary formalism took place during a visit to TRIUMF in 1978, and the author wishes to thank E. Vogt for that opportunity.

References

1. A Proposal to the Department of Energy for a High Intensity Los Alamos Neutrino Source (Los Alamos, January 15, 1982).
2. T. W. Donnelly and R. D. Peccei, Phys. Reports 50, 1 (1979).
3. T. W. Donnelly et al., Phys. Lett. 49B, 8 (1974).
4. T. W. Donnelly and R. D. Peccei, Phys. Lett. 65B, 196 (1976).
5. T. W. Donnelly and J. D. Walecka, Nucl. Phys. A274, 368 (1976).
6. T. W. Donnelly (to be published).
7. T. W. Donnelly and W. C. Haxton, At. Data and Nucl. Tables 23, 103 (1979); 25, 1 (1980).
8. H. Chen and F. Reines, UCI-Neutrino Report No. 31 (1979).
9. T. W. Donnelly, "Highlights of Nuclear Physics with Neutrinos", Part of the Los Alamos Neutrino Workshop (June, 1981).
10. R. M. Barnett, Phys. Rev. D14, 2990 (1976).

the most natural uncorrelated shell model configurations[†]:

[†]For the ^2H case, a $^3S_1 + {}^3D_1$ ground state is also considered (see below).

$$^2H \leftrightarrow (1s_{1/2})^2 \leftrightarrow {}^3S_1 \qquad J^\pi T, M_T = 1^+ 0,0$$

$$^4He \leftrightarrow (1s_{1/2})^4 \qquad 0^+ 0,0$$

$$^{12}C \leftrightarrow (1s_{1/2})^4 (1p_{3/2})^8 \qquad 0^+ 0,0$$

$$^{16}O \leftrightarrow (1s_{1/2})^4 (1p_{3/2})^8 (1p_{1/2})^4 \qquad 0^+ 0,0$$

$$^{27}Al \leftrightarrow (1s_{1/2})^4 (1p_{3/2})^8 (1p_{1/2})^4 (1d_{5/2})^{11} \qquad \tfrac{5}{2}^+ \tfrac{1}{2}, -\tfrac{1}{2}$$

$$^{40}Ca \leftrightarrow (1s_{1/2})^4 (1p_{3/2})^8 (1p_{1/2})^4 (1d_{5/2})^{12} \times (2s_{1/2})^4 (1d_{3/2})^8 \qquad 0^+ 0,0$$

$$^{56}Fe \leftrightarrow (1s_{1/2})^4 (1p_{3/2})^8 (1p_{1/2})^4 (1d_{5/2})^{12} \times (2s_{1/2})^4 (1d_{3/2})^8 (1f_{7/2})^8_n (1f_{7/2})^6_p \times (2p_{3/2})^2_n \qquad 0^+ 2,-2$$

In fact, because of the dominance of the coherent isoscalar vector current monopole contribution (αA^2), for all but the lightest nuclei the cross sections come mainly from matrix elements of the single operator $\hat{M}_{00;00}$. This is similar to the situation for elastic electron scattering where the monopole (charge) cross section involves the same operator. This dominance of the $\mathcal{J} = \mathcal{T} = 0$ operator of course is exact for nuclei having J = T = 0 (^4He, ^{12}C, ^{16}O, ^{40}Ca here). For the cases of ^{27}Al and ^{56}Fe in the present work only the monopole operator ($\mathcal{J} = 0$) is used, however both isoscalar ($\mathcal{T} = 0$) and isovector ($\mathcal{T} = 1$) contributions are included (although

the former still dominates). For the case of the deuteron (^{2}H), being too light to invoke the dominance of the monopole contribution with safety, all allowed multipoles are included (see below).

With these assumed ground-state configurations it is straightforward to calculate the necessary one-body density matrix elements using Eq. (12). For single-particle matrix elements the tables in Ref. 7 are employed and in particular, in the present work, since harmonic oscillator radial wave functions are adequate for the range of momentum transfers appropriate at these (intermediate) neutrino energies, they are used throughout. Finally, having the model one-body density matrix elements and the necessary single-particle matrix elements of the complete set of multipole operators listed in Eq. (6), it is possible to obtain the many-body matrix elements required using Eq. (11) and hence the neutrino and anti-neutrino cross sections using Eq. (1) for some assumed set of gauge model couplings $\beta_V^{(\mathcal{J})}$, $\beta_A^{(\mathcal{J})}$, $\mathcal{J} = 0,1$. The one free parameter, the oscillator parameter b, is then determined by fitting experimental elastic (charge) electron scattering form factors using the same assumptions for the ground-state shell model configurations. The values of b so obtained are listed in Table I.

With this brief discussion of the basic formalism we proceed to specific results in Sections II and III.

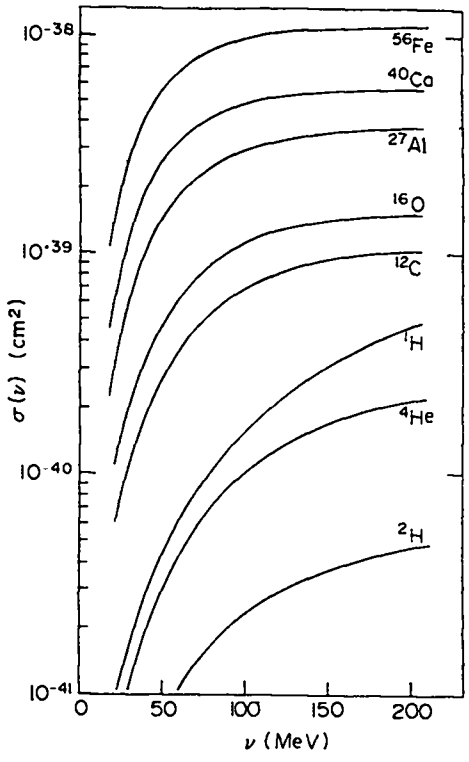

Fig. 1. Total Neutrino cross sections $\sigma(\nu)$ versus neutrino energy ν using the standard model.

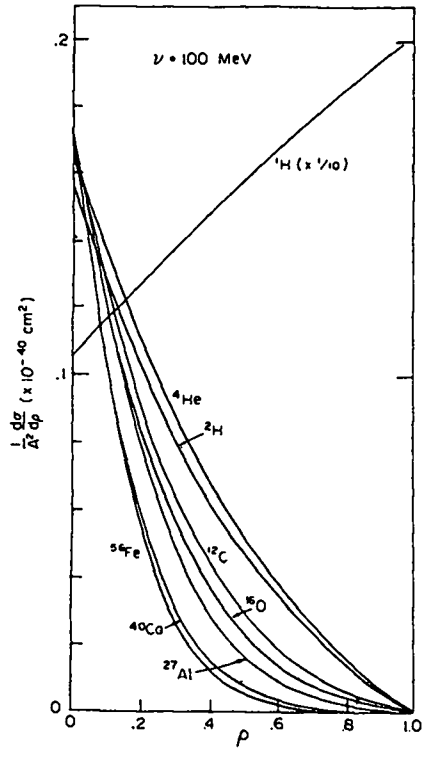

Fig. 2a. Differential neutrino cross sections $A^{-2}d\sigma/d\rho$ versus ρ, where $\rho = \omega/\omega_M$ with ω the nuclear recoil energy and ω_M its maximum value (a function of neutrino energy ν and nuclear mass, see Table II). The results here are for ν = 100 MeV, obtained using the standard model.

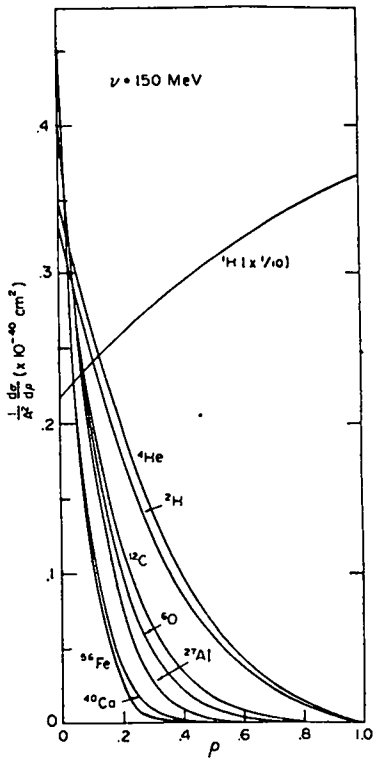

Fig. 2b. As for Fig. 2a, but with ν = 150 Mev.

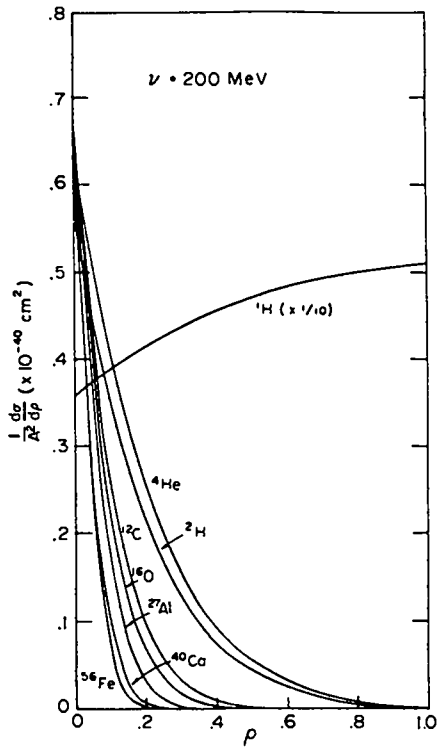

Fig. 2c. As for Fig. 2a, but with ν = 200 MeV.

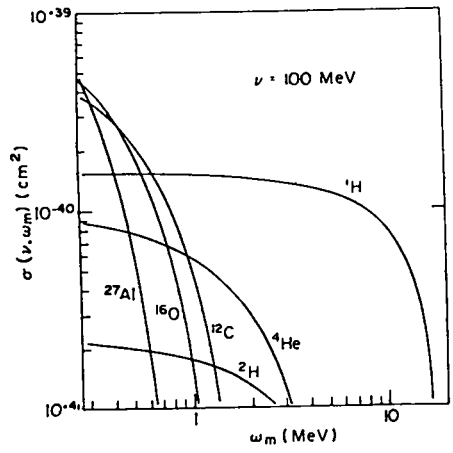

Fig. 3a. Integrated neutrino cross sections $\sigma(\nu,\omega_m) = \int_{\omega_m}^{\omega_M} \frac{d\sigma}{d\omega} d\omega$ versus ω_m, where ω is the nuclear recoil energy, ω_M is its maximum value (a function of neutrino energy ν and nuclear mass, see Table II), and ω_m is a variable lower limit to the integral. The results here are for ν = 100 MeV, obtained using the standard model.

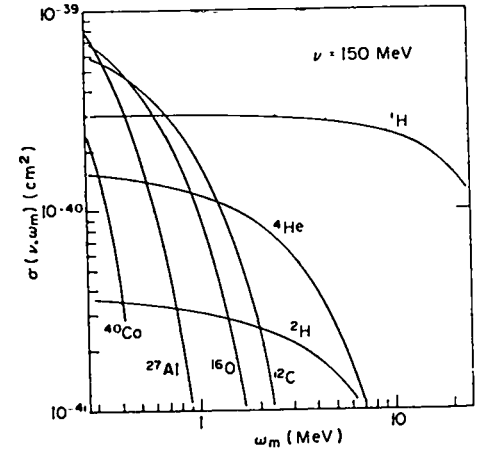

Fig. 3b. As for Fig. 3a, but with ν = 150 MeV.

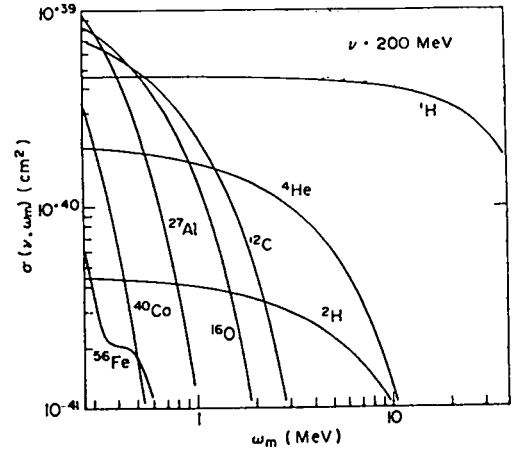

Fig. 3c. As for Fig. 3a, but with ν = 200 MeV.

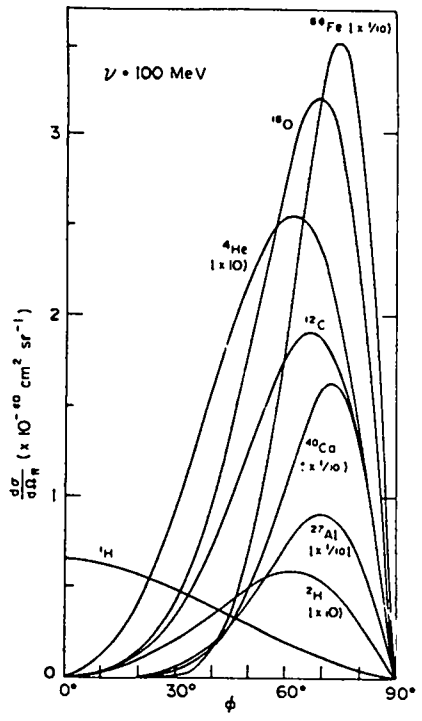

Fig. 4a. Differential neutrino cross sections $d\sigma/d\Omega_R$ (differential in nuclear recoil solid angle) versus ϕ, the angle between the incident neutrino and the recoiling nucleus. The results here are for ν = 100 MeV, obtained using the standard model.

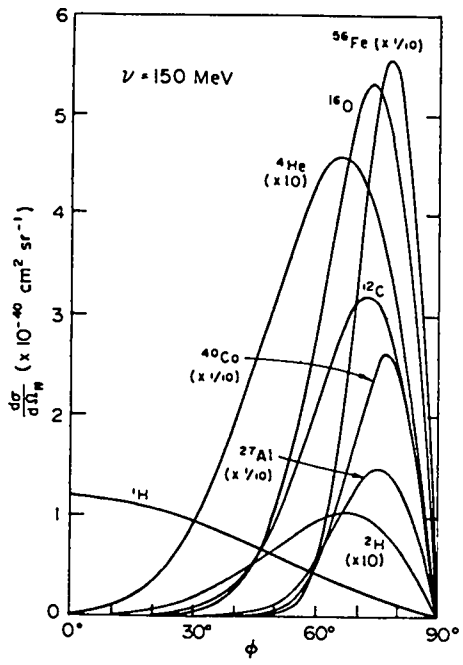

Fig. 4b. As for Fig. 4a, but with ν = 150 MeV.

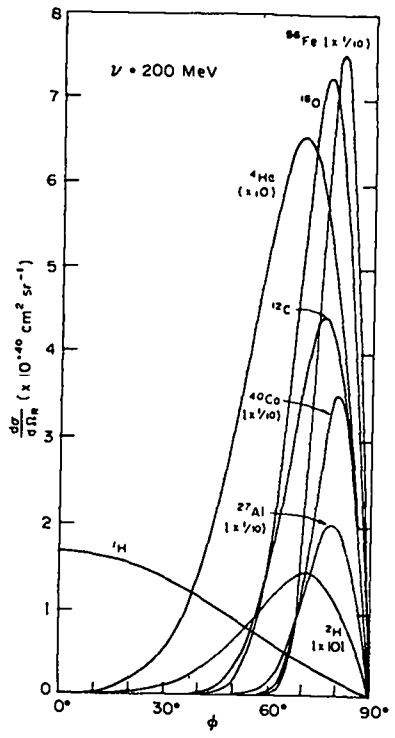

Fig. 4c. As for Fig. 4a, but with ν = 200 MeV.

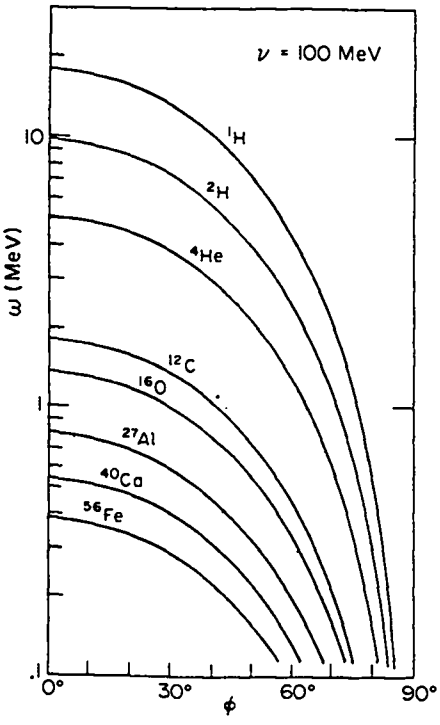

Fig. 5a. Nuclear recoil energy ω versus ϕ, the angle between the incident neutrino and the recoiling nucleus, for ν = 100 MeV.

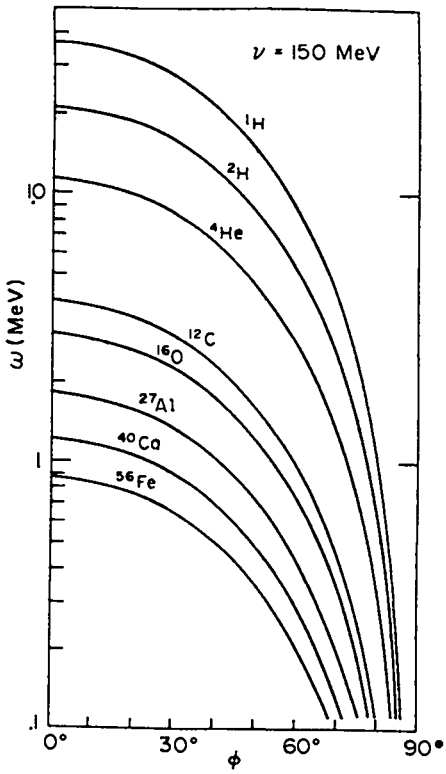

Fig. 5b. As for Fig. 5a, but with ν = 150 MeV.

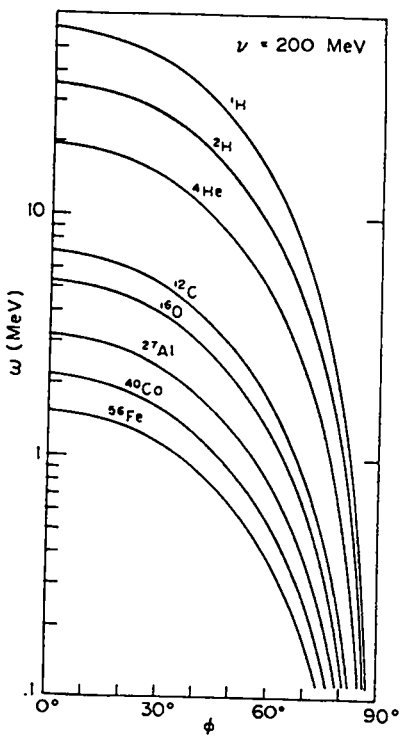

Fig. 5c. As for Fig. 5a, but with ν = 200 MeV.

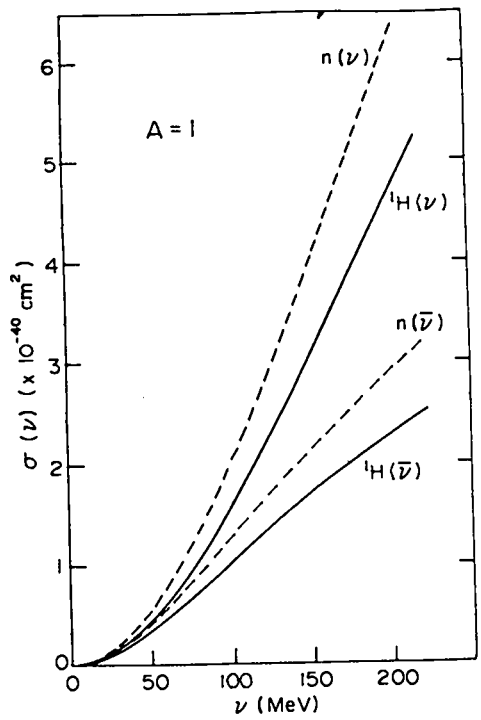

Fig. 6. Total neutrino and anti-neutrino cross sections $\sigma(\nu)$ versus neutrino or anti-neutrino energy ν for the neutron and proton (^1H) using the standard model.

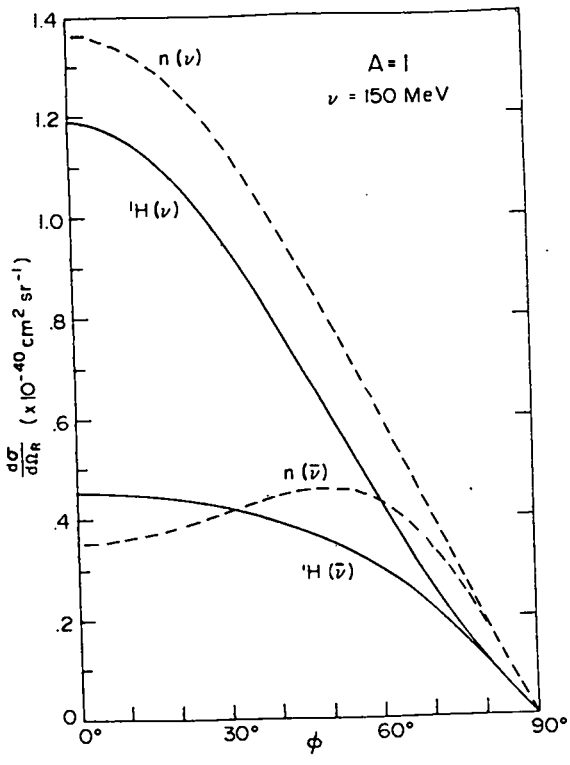

Fig. 7. Differential neutrino and anti-neutrino cross sections $d\sigma/d\Omega_R$ (differential in recoil solid angle) versus ϕ, the angle between the incident neutrino (or anti-neutrino) and the recoiling neutron or proton (^1H). The results here are for neutrino or anti-neutrino energy ν = 150 MeV, obtained using the standard model.

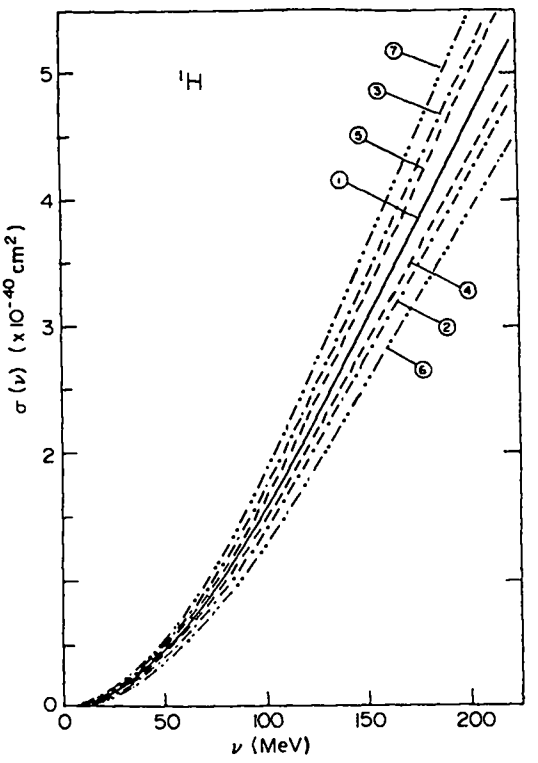

Fig. 8. Total neutrino cross sections $\sigma(\nu)$ versus neutrino energy ν for the proton (^{1}H) using the seven sets of gauge model couplings given in Table III numbered 1-7).

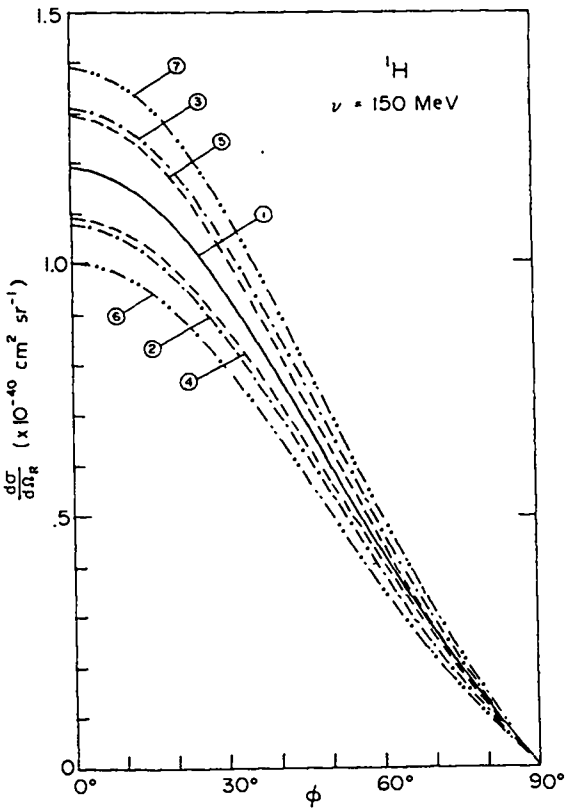

Fig. 9. Differential neutrino cross sections $d\sigma/d\Omega_R$ (differential in recoil solid angle) versus ϕ, the angle between the incident neutrino and the recoiling proton (^{1}H). The results here are for the seven sets of gauge model couplings given in Table III (numbered 1-7).

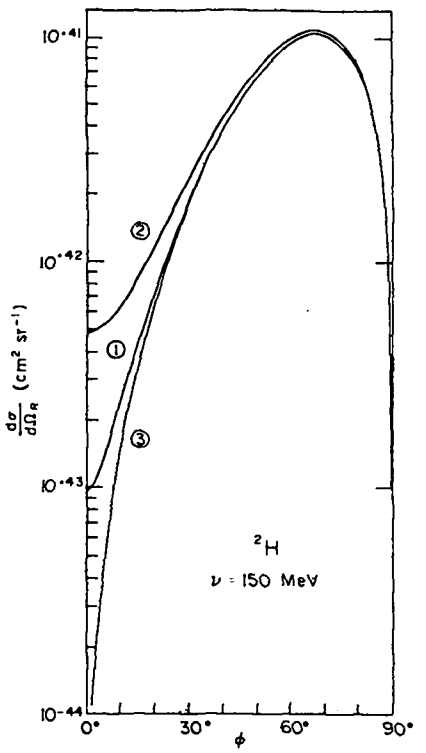

Fig. 10. Differential neutrino cross sections $d\sigma/d\Omega_R$ (differential in recoil solid angle) versus ϕ, the angle between the incident neutrino and the recoiling deuteron (^2H). The results here are for the three sets of gauge model couplings given in Table III numbered 1-3. For anti-neutrinos, interchange the results for sets 2 and 3.

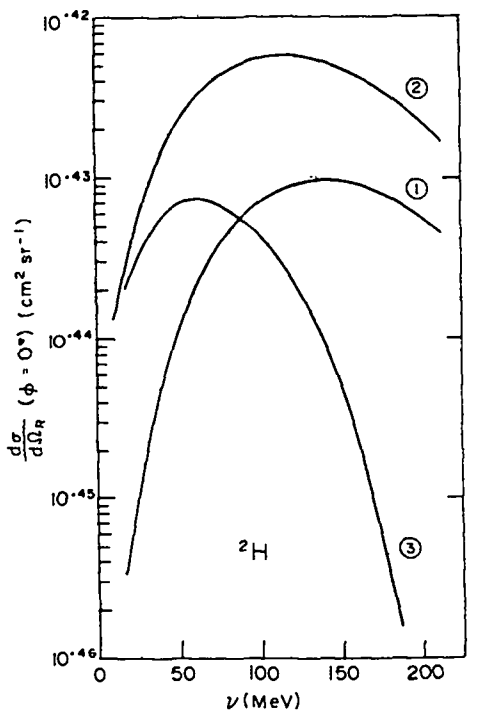

Fig. 11. Differential neutrino cross section $d\sigma/d\Omega_R$ at recoil angle $\phi = 0^o$ versus neutrino energy ν for the deuteron (^2H). The results here are for the three sets of gauge model couplings given in Table III numbered 1-3. For anti-neutrinos, interchange the results for sets 2 and 3.

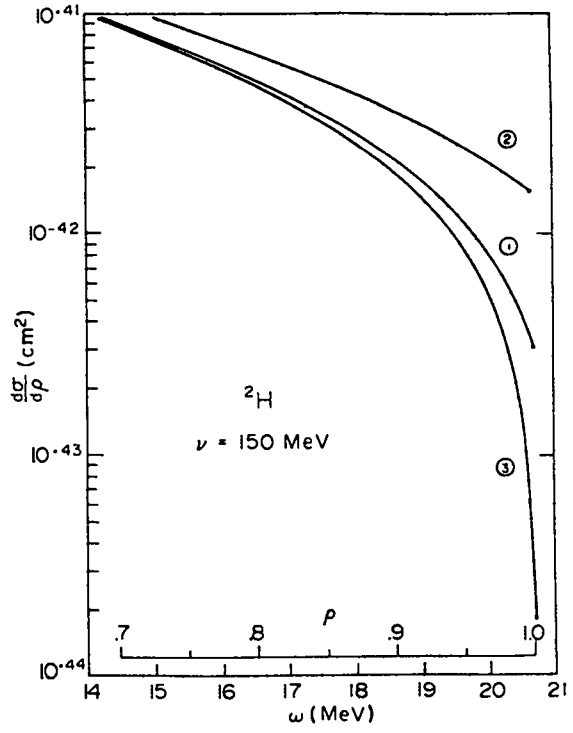

Fig. 12. Differential neutrino cross sections $d\sigma/d\rho$ versus ρ, where $\rho = \omega/\omega_M$ with ω the deuteron (^2H) recoil energy and ω_M its maximum value (ω_M = 20.68 MeV for neutrino energy ν = 150 MeV, see Table II). The results here are for the three sets of gauge model couplings given in Table III numbered 1-3. For anti-neutrinos, interchange the results for sets 2 and 3.

Printed in the United States of America
Available from
National Technical Information Service
US Department of Commerce
5285 Port Royal Road
Springfield, VA 22161

Microfiche (A01)

Page Range	NTIS Price Code	Page Range	NTIS Price Code	Page Range	NTIS Price Code	Page Range	NTIS Price Code
001-025	A02	151-175	A08	301-325	A14	451-475	A20
026-050	A03	176-200	A09	326-350	A15	476-500	A21
051-075	A04	201-225	A10	351-375	A16	501-525	A22
076-100	A05	226-250	A11	376-400	A17	526-550	A23
101-125	A06	251-275	A12	401-425	A18	551-575	A24
126-150	A07	276-300	A13	426-450	A19	576-600	A25
						601-up*	A99

*Contact NTIS for a price quote.

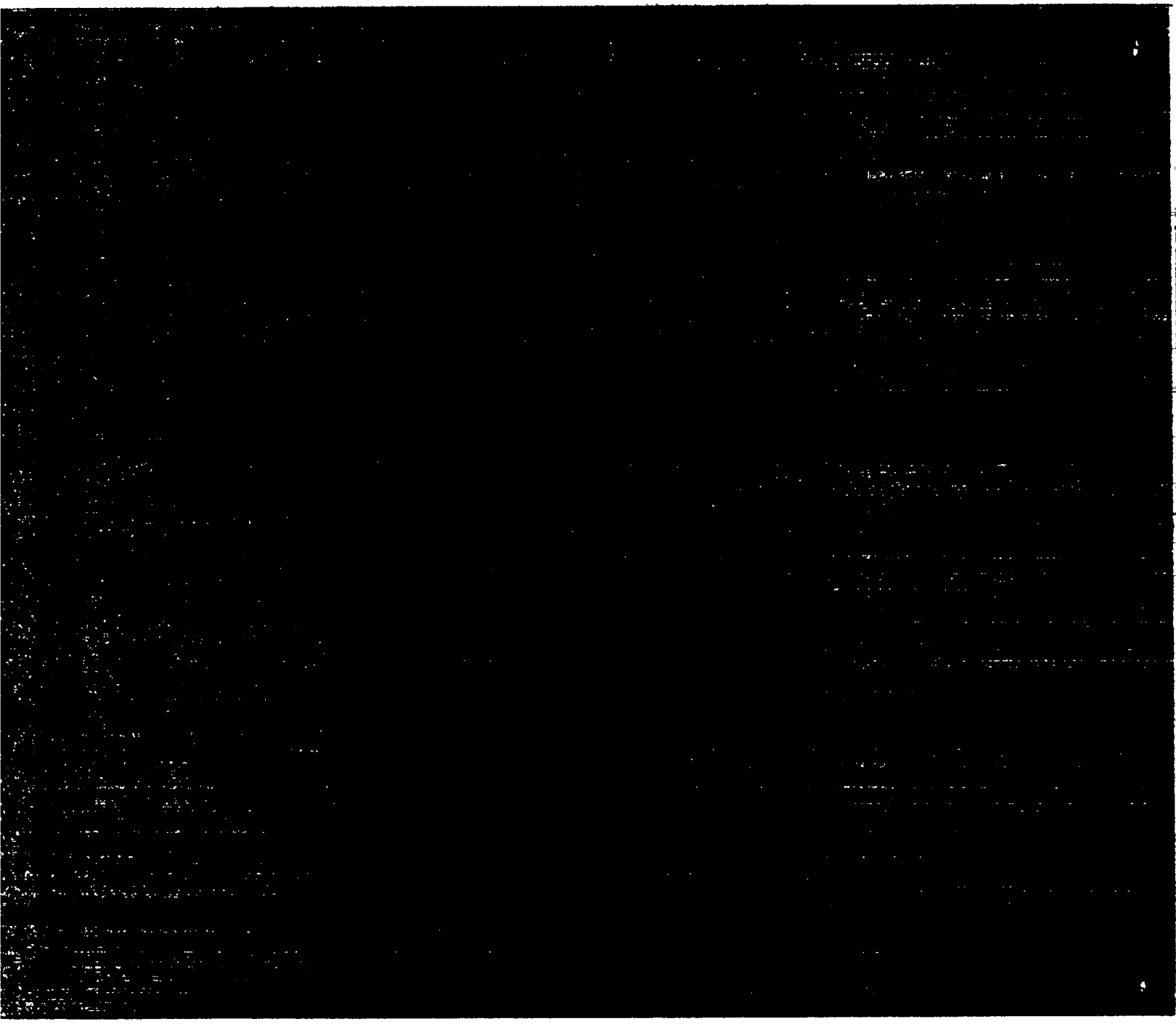

Los Alamos